1967

The crystal structure determinations of OP(OCH2)3CCH3 and a hydrolysis product of PO3C6H9

Dale Meyers Nimrod
Iowa State University

NIMROD, Dale Meyers, 1940-

THE CRYSTAL STRUCTURE DETERMINATIONS OF $OP(OCH_2)_3CCH_3$ AND A HYDROLYSIS PRODUCT OF $PO_3C_6H_9$.

Iowa State University, Ph.D., 1967
Chemistry, physical

University Microfilms, Inc., Ann Arbor, Michigan

THE CRYSTAL STRUCTURE DETERMINATIONS OF $OP(OCH_2)_3CCH_3$ AND A HYDROLYSIS PRODUCT OF $PO_3C_6H_9$

by

Dale Meyers Nimrod

A Dissertation Submitted to the
Graduate Faculty in Partial Fulfillment of
The Requirements for the Degree of
DOCTOR OF PHILOSOPHY

Major Subject: Physical Chemistry

Approved:

Signature was redacted for privacy.

In Charge of Major Work

Signature was redacted for privacy.

Head of Major Department

Signature was redacted for privacy.

Dean of Graduate College

Iowa State University
Of Science and Technology
Ames, Iowa

1967

TABLE OF CONTENTS

INTRODUCTION

The chemistry of bicyclic alkoxy phosphorus compounds of the types

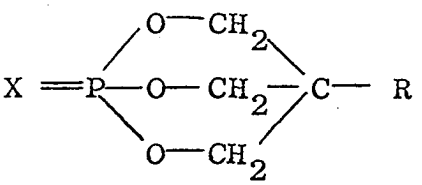

I

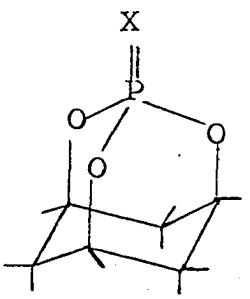

II

where X = nothing, O or S, and R = CH_3, C_2H_5 or n-C_5H_{11}, has been the subject of considerable study since the compounds were first reported. The phosphite forms have received the most attention due to their strong ligand properties. Interestingly high P = O stretching frequencies have been observed in the infrared spectra of the phosphate forms. The mechanisms for opening the caged structures with alkyl halides, water and halogens have been compared and contrasted. Nuclear magnetic resonance and dipole moment experiments as well as infrared studies have been used as tools for postulating structural features of the compounds and their derivatives.

The crystal structure determinations of two of these compounds were undertaken by means of x-ray diffraction to

confirm the postulated configurations and to measure quantitatively their various structural features. The compounds examined in this study were the 4-methyl-1-oxide derivative of I, 1-oxo-4-methyl-2,6,7-trioxa-1-phosphabicyclo[2.2.2]octane, hereafter referred to as phos-oxide, and one of the two isomers of the acid-catalyzed hydrolysis of the phosphite form of II, 3-α-oxo-3-β-hydrido-7-β-hydroxy-2,4-dioxa-3-phosphabicyclo[3.3.1]nonane, hereafter referred to as isomer A.

In addition the space group determination and its structural implications of the crystal structure of the related bicyclic phosphorus compound, $OP(N(CH_3)CH_2)_3CCH_3$ (1-oxo-2,6,7-trimethyl-4-methyl-2,6,7-triaza-1-phosphabicyclo[2.2.2]octane) are reported in Appendix A.

In the course of automating a four-circle x-ray diffractometer by means of a computer system an algorithm for maximizing and centering a general reflection was developed. The mathematical expressions necessary for its implementation were derived and are presented in Appendix B.

THE STRUCTURE OF $OP(OCH_2)_3CCH_3$

Introduction

Bicyclic alkoxy phosphites of the types $P(OCH_2)_3CR$, where $R=CH_3$, C_2H_5 and $n\text{-}C_5H_{11}$, and $P(OCH)_3(CH_2)_3$ have been shown to function as excellent electron donors in a variety of conditions and have attracted a good deal of attention since their discoveries (1,2). The unoxidized parent of the subject of this structure determination, $P(OCH_2)_3CCH_3$, has been a particularly strong ligand. In contrast with comparable open chain trialkyl phosphites which form complexes with only the heavy transition metals such as Pt(II) and a few post transition metals such as Hg(II), $P(OCH_2)_3CCH_3$ forms complexes with first row transition metal ions (3) and with transition metal carbonyls (4,5) as well as stable adducts with boron containing Lewis acids (6).

The H^1 and P^{31} n.m.r. spectra of both the phosphite and the phosphate were investigated by Verkade and King (7) and gave firm support to the postulated bicyclic configuration. The simplicity of the proton spectra, consisting of a methyl singlet and a methylene doublet, could be accounted for only with the presence of a threefold axis through the molecule. The P^{31} resonance and coupling also supported the configuration.

The greater donor ability of the bicyclic phosphite is undoubtedly due to the reduction of steric hinderance between the ligands in a complexed system as well as between the ligand itself and the metal to which it is coordinated when the alkoxy groups are constrained in the manner in this cyclic ring system.

In spite of the fact that the molecular configuration had been deduced, the x-ray structure analysis of phos-oxide was undertaken for several reasons. First of all, no other bicyclic phosphate structure determinations have been reported. The structural parameters of the phosphate are expected to closely approximate the structural features of the coordinated phosphite in transition metal complexes and adducts which have been and are under study. Quantitative estimates of bond angles on the basis of *n.m.r.* spectra have been made and should be tested. The structural parameters of phosphonium cations of the type $[RP(OCH_2)_3CCH_3]^+$ (8) and of phosphonium intermediates in the Michaelis-Arbuzov reactions of $P(OCH_2)_3CCH_3$ (9) should be closely approximated by the structure of phos-oxide. In addition the structural parameters were sought to see if the lack of extraction properties of the related bicyclic phosphate, $OP(OCH_2)_3CC_5H_{11}$, could be understood (10). Related to the last point is the question concerning the reason for the very high P=O infrared stretching frequencies observed in the bicyclic phosphates and their implications in terms of bonding.

Experimental

The preparation of the unoxidized form of phos-oxide was accomplished by refluxing trimethyl phosphite with the proper alcohol (2-hydroxymethyl-2-methyl-1,3-propanediol) (8).

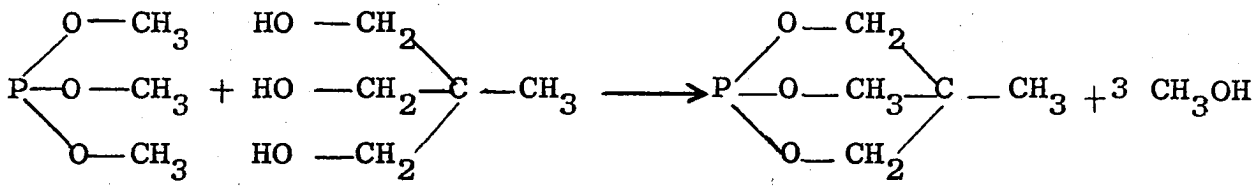

Oxidation to the phosphate takes place with the addition of hydrogen peroxide to a solution of the phosphite in absolute ethanol (1).

Crystals of phos-oxide suitable for x-ray analysis were obtained by slow sublimation at 100°C inside a water cooled sublimation apparatus. The long, needle-like, soft crystals which formed on the wall of the apparatus were removed and severed with a razor blade into approximate cubes. Torsional distortion invoked by the stress of the cutting process was a problem, but the degree of distortion could be observed by examining Weissenberg photographs for drawn-out spots along the axis of rotation (the crystal needle axis). A good single crystal which apparently was not stressed was obtained by this procedure and was the crystal used for the intensity measurements. Later attempts, however, to get suitable fresh crystals by this method for the purpose of obtaining

accurate lattice constants and for remeasuring a portion of the intensity data were not successful.

Other attempts to grow suitable crystals included sublimation inside an evacuated seven millimeter glass tube. Heat was supplied in one case with a 500 watt heat bulb and in another case with a coil of resistance wire wrapped around the tube so as to make a smooth temperature gradient. Considerable difficulty, however, was encountered in attempting to remove the crystals without damaging them since they tended to adhere firmly to the glass wall. Attempts to grow suitable crystals from methanol, ethanol, butanol, and dioxane solutions were also unsuccessful.

The crystals used for the space group determination as well as for the intensity gathering process were glued onto the end of a glass fiber with the needle axis being coincident with the mounting axis. The long axis of the unit cell, c, is coincident with the external needle axis.

Both Weissenberg and precession photographs were taken with CuKα radiation. The observed diffraction symmetry was m m m (orthorhombic). Systematic conditions for non-extinction were observed to be as follows:

$hk\ell$: no conditions

$h0\ell$: $\ell=2n$

00ℓ: $\ell=2n$ (redundant)

$h00$: $h=2n$.

The first three conditions are compatable with space groups Pmcm [Pmma as defined in the International Tables (11)], P2cm (Pma2) and $Pmc2_1$. The third condition is not required by the space group; the implication of its presence will be discussed later.

Measurements for the determination of the lattice parameters of phos-oxide were taken from several sources. In addition to measurement made on the Weissenberg and precession photographs (CuKα radiation) a General Electric single crystal orienter x-ray unit was used with both MoKα and CrKα radiation. Three more measurements were taken using a Hilger and Watts four-circle x-ray diffractometer using MoKα radiation. The full circle capabilities allowed the measurement of the same reflection in several equivalent orientations. The data were refined and the lattice parameters and their estimated standard deviations were calculated by means of a least-squares lattice constant refinement program of Williams (12). The parameters and their standard deviations taken from the variance-covariance matrix are as follows:

$a = 6.736 \pm 0.003$ A

$b = 5.960 \pm 0.017$ A

$c = 17.768 \pm 0.004$ A

volume = 713.3 A^3.

Four molecules (molecular weight = 164.1) per unit cell give a calculated density of 1.53 gms/cm^3. The observed density, obtained by means of flotation observations of single crystals in mixtures of benzene and carbon tetrachloride, of 1.51 gms/cm^3 agrees favorably.

Two experiments were carried out in an effort to elucidate the presence or absence of a center of symmetry in the space group. Maurice (13) described a test in 1930 whereby a single crystal is immersed in a bath of liquid nitrogen. Non-centrosymmetric crystals may become electrostatically charged, and upon removal, exhibit whisker-like crystals of ice following the lines of electric force in the same manner in which iron filings follow the magnetic lines of force around a magnet. On the other hand, since no electrostatic charge can be built up in centrosymmetric crystals, the ice forms an even coat on the crystal.

The largest single crystal of phos-oxide that could be found was glued to the end of a fine thread and suspended in a bath of liquid nitrogen. A microscope, previously focused on the crystal, was used to observe the icing when the liquid nitrogen was removed. It appeared as if the icing formed an even coating on the crystal. Control experiments were run with α-quartz, a well known acentric crystal, upon which ice formed in a pattern definitely following the lines of the electric field. Positive tests (a smooth coating) were

obtained for two known centric crystals. It was recognized, however, that although a positive test for pyroelectricity is a valid indication of a non-centrosymmetric crystal, the lack of a display of pyroelectricity cannot be taken as a true indication for the presence of a center of symmetry in the crystal. No space group implications, therefore, could be made on the basis of this test.

A second experimental test for pyroelectricity as described by Wheatley (14) was attempted in which a powdered sample is placed in an anodized aluminum spoon to which liquid nitrogen is added. As the nitrogen evaporates the crystals form a ball which either collapses or remains together depending upon whether the crystals are centrosymmetric or non-centrosymmetric respectively. The phos-oxide crystals were too soft and waxy to form a suitable powder, however, and no conclusions could be made from this approach, either.

Examination of the symmetry elements of the three possible space groups coupled with a knowledge of the number of molecules per unit cell, a well-grounded proposal for the molecular configuration, and the non-required systematic extinctions in the h00 data, led to the assignment of space group $Pmc2_1$. That the extra systematic extinction does not correspond to a twofold screw axis in the x direction can be seen from group theory. Since the product of any two elements of the group must be a member

of the group, and since a c glide in the b direction is known to exist, the product of the operations of the screw axis and the glide plane must be in the group. A c glide in the b direction takes a general point, (x,y,z), to (x,-y, 1/2 + z). A twofold screw axis in the a direction takes the result to (x + 1/2, y, 1/2 - z) which is the point reached by operating on (x,y,z) with an a glide in the c direction when the glide plane is located at z = 1/4. Now an a glide in the c direction would result in systematic extinctions in the hk0 data for all reflections for which h was odd. Since these conditions were clearly not met in the film data, it was concluded the h00, h=2n condition was due to a special arrangement of the molecules within the cell.

In order for the four molecules of phos-oxide to crystallize in a cell with space group symmetry Pmcm, which has eight general positions, the molecules must occupy the fourfold set of special positions on the mirrors. Since the molecule was assumed to have C_{3v} point group symmetry, this arrangement may be made. Of the two mirrors only one (to which a is normal) may be used when one considers the size of the molecule in connection with the dimensions of the two mirrors as defined by the lattice constants. Either of the a mirrors (x=0 and x=1/2) but not both (assuming no disorder) may be used. Since the greatest portion

(49 electrons) of the total scattering ability (77 electrons) lies on the mirror, and since the mirrors are in positions for which the geometrical part structure factor expression allows full contribution of the scattering factor, the intensities of the h00 reflections will be completely dominated by the scatterers on the mirrors. Their intensities, therefore, will fall off in intensity in the same manner that the scattering factor curves decrease with sin θ/λ. It may be seen, then, that if there were disorder in the crystal which would statistically use the x=0 mirror half the time and the x=1/2 mirror the other half, the scattering from one mirror would be 180° out of phase with the scattering from the other for h00 reflections, $h \neq 2n$, and the extra systematic extinctions would thus arise. It also appears that placement of all four molecules on the 6 x 18 A mirror is not a very energetically favorable arrangement. Therefore, assignment of Pmcm would imply a disordered arrangement which should be considered only if no ordered structure could be found.

The fourfold set of general positions would have to be used if the space group P_2cm were assigned because the only mirror contained in this space group is of dimensions 6 x 8 A, and it was felt that that was not enough area to incorporate two molecules. Therefore, assignment P_2cm is impossible since the structure factor expression for atoms

in general positions could not yield systematic h00 extinctions.

Assuming no disorder, the space group assignment was made to $Pmc2_1$. This non-centrosymmetric space group also has four general positions, but unlike P2cm its mirrors (one at x=0, the other at x=1/2) are parallel to c and are, therefore, of dimensions 7 x 18 A and are large enough to accommodate two molecules each. If the molecules were so arranged the situation would be that of the disorder case of space group Pmcm, and the systematic h00 extinctions could then be accounted for. Such an arrangement was assumed and was subsequently proven correct.

It is noted that the pair of symmetrically related molecules on the x=0 mirror are crystallographically independent of the pair on the x=1/2 mirror. This arrangement is desired on the part of the crystallographer (for small problems) because although more structural parameters need to be determined than in the case where there is only one molecule per asymmetric unit, there are twice as many chemically equivalent distances and angles which would be expected to lead to more accurate estimations of parameter errors.

A full octant of x-ray diffraction intensity data was gathered at room temperature with zirconium filtered molybdenum radiation from an approximately parallelepiped crystal of dimensions 0.13 x 0.23 x 0.25 mm. A General

Electric XRD-5 x-ray unit equipped with a single crystal orienter and a scintillation counter was used to measure the intensities of the reflections. A 100 second, 1.67° - 2θ moving-crystal-moving-counter scan technique (15) was employed. The same 2θ range for each reflection was scanned with an omega offset of 1.8° for background correction. The data taking began with a 3.0° take-off angle, but when peaks started overlapping, the take-off angle was reduced to 1°, and the data gathering was started again from the beginning. The reduction of the take-off angle gave the desired result of eliminating the peak overlap program. It is felt, however, that more serious problems were encountered because of the reduced angle when the crystal apparently shifted slightly. The collected data is thought to suffer slightly because of the lack of special precautions that should have accompanied the reduction of the angle.

Nearly all of the intensities of the 1600 reflections within a 2θ sphere of 65° were measured, but only those below 55°, 2θ were generally distinguishable from background and were used in the refinement.

Three standard peaks (0,6,0; 1,0,14; 0,0,16) were measured periodically throughout the data taking process for monitoring decomposition and crystal shifting. A general ten per cent decrease in intensity was observed. The intensities were corrected accordingly. Correction of the

intensities for lost counts due to non-linearity in the counting chain was made on the basis of 21 of the strongest reflections whose intensities were measured at one milliamp tube current as well as at the regular current (18 ma). The ratio of the intensities of the peaks at each setting were plotted against the measured peak at the data taking current. It was observed that the ratio became constant below a certain counting rate. All peaks above this counting rate were corrected according to the plot.

In addition, the intensities were corrected for the usual Lorentz-polarization

$$LP = \frac{1 + \cos^2 2\theta}{2 \sin 2\theta}$$

and also for non-characteristic ("streak") radiation. Since the non-characteristics radiation is a function of the mosaic character of the crystal under observation as well as the characteristics of the x-ray tube and the applied voltages, its correction is based on its experimentally measured distribution. The method and expressions derived by Benson and Fitzwater[*] were used to correct the intensities of the reflections of order three or greater. A discussion of streak and its correction which is essentially the same

---

[*]J. E. Benson and D. R. Fitzwater, Ames, Iowa, Ames Laboratory, U.S. Atomic Energy Commission. Streak correction. Private Communication. 1964.

as that used has been reported by Williams and Rundle (16).

An estimate of the standard deviation of the intensity for each reflection was computed by means of the following expression:

$$\sigma_I^2 = TC + Bg + (P_T TC)^2 + (P_B Bg)^2 + (P_S St)^2.$$

TC, Bg and St refer to total counts, background and streak, respectively. The first two terms represent statistical uncertainty in the peak and background measurements. P_T, P_B and P_S refer to estimated relative errors in the measurement or calculations of peak, background and streak correction. For those reflections for which the corrected intensity was greater than zero, a standard deviation for the observed structure factor was computed by means of the expression

$$\sigma = \frac{\sigma_I Fo}{2I}$$

where I is the corrected intensity and Fo is the observed structure factor ($Fo = (I/LP)^{1/2}$). The rest of the unobserved reflections were given σ_F's which were representative of the small but non-zero Fo's.

Structure Determination

The space group $Pmc2_1$ is polar with respect to z, thereby permitting an arbitrary origin in that direction. Assuming that the molecules lie on the mirrors at $x=0$ and $x=1/2$ by the reasoning discussed earlier, a phosphorus of one of

the molecules, at the outset, could be fixed with respect to x and z. A Patterson map was computed using all of the data by means of a Fourier summation program of Ledet (17). Unfortunately, the phos-oxide structure did not lend itself well to conventional Patterson techniques in that, first of all, there are numerous interatomic vectors which are parallel and which manifested themselves in terms of overlapping, smeared out peaks on the Patterson map. Secondly, because of the placement on the mirrors, not only are most of the interatomic vectors oriented in the y,z plane, but so also are most of the intermolecular vectors between the atoms of a molecule and its symmetrically related mate (also on the same mirror). The Harker line, (0, y, 1/2), containing all of the P-P', O-O' and C-C' vectors (the primed and the unprimed atoms are related by the c glide in the b direction), for example, was seen to contain a total of two large, smeared out peaks with a hint of a shoulder on one of the peaks. In an effort to make more use of the Patterson function the data was modified by means of a sharpening function and program of Granoff and Jacobson[*]. This modification is in the form of multiplicitive factors, applied to each structure factor value, which in

---

[*]B. Granoff and R. A. Jacobson, Ames, Iowa, Ames Laboratory, U.S. Atomic Energy Commission. A data sharpening program. Private Communication. 1964.

essence straightens out the scattering factor curves with respect to sin θ/λ as would be the case if the x-rays were scattered by point sources instead of finite sized distributions of scatterers. The result, in terms of the Patterson function, is sharper, less diffuse peaks. Still, however, there was a great deal of overlap.

The same overlap problem was felt to be the cause of the prevention of obtaining useful interpretations of attempted superposition techniques. The first step in the solution of the structure was finally made by proposing molecular orientations, which in conjunction with packing considerations, would give rise to a maximum number of vectors in a direction that would account for the very large peaks on the (0, y, 1/2) Harker line and still be consistant with the other large peaks.

Once the orientations of the molecules were proposed, the two phosphorous locations were postulated and refined by least-squares techniques. The assumed molecular structure was used to propose the terminal oxygen sites and finally the other mirror-containing atoms. Further least-squares refinement and subsequent Fourier electron density syntheses (17) led to the inclusion of the remainder of the atoms.

Refinement of the structure was accomplished by means of a full matrix least-squares program of Fitzwater* which minimized the quantity, $\Sigma w(|Fo|-|Fc|)^2$, where $w = \frac{1}{\sigma_F^2}$. Hartree-Fock-Slater atomic scattering factor tables (18) were employed in the calculation of the structure factors. Anisotropic thermal parameters were eventually given and varied for each atom. It was felt that the quality of the data did not warrant the inclusion of hydrogen atoms.

Near the end of the refinement the data was ordered in terms of decreasing magnitude of Fo and a structure factor calculation was made in which an R-factor summary was computed every 50 reflections. A plot of the weighted R-factor vs. the average Fo of the set showed a linear decline in the R-factor with the decrease in Fo. It was assumed that with the proper weighting scheme the weighted R-factor would be constant for portions of data analysed in any significant systematic fashion (19). A linear correction which tended to remove the dependence was applied to the σ_F's. It is felt that the standard deviations of the parameters were meaningfully improved with this adjustment.

The final value of the residual discrepancy index or R-factor

---

*D. R. Fitzwater, Ames, Iowa, Ames Laboratory, U.S. Atomic Energy Commission. A crystallographic least-squares program for the IBM 7074. 1963.

$$R = \frac{\Sigma||Fo|-|Fc||}{\Sigma|Fo|}$$

for relating 108 positional and thermal parameters to 781 observed reflections is 0.082.

The weighted R-factor

$$R_{wt} = \frac{\Sigma||Fo/\sigma|-Fc/\sigma||}{\Sigma|Fo/\sigma|}$$

is 0.078. The total 1191 reflections used in the refinement gave an unweighted R-factor of 0.0121 and a weighted R-factor of 0.105. A list of these calculated and observed structure factors is given in Figure 1. The final positional and thermal parameters and their standard errors from which the calculated structure factors were computed are listed in Table 1.

The Structure

A drawing of the molecular structure found for phos-oxide with accompanying pertinent interatomic distances and angles is given in Figure 2. The distances and angles and their standard errors were computed on the basis of the complete variance-covariance matrix of the last least squares cycle by means of a function and error program of Busing, Martin and Levy (20). The values of the distances and angles shown in Figure 2 are averages of the chemically equivalent but crystallographically independent structural features of the two molecules. A list of the individual interatomic

Figure 1. Comparison of calculated and observed structure factors for $OP(OCH_2)_3CCH_3$ based on the structural parameters given in Table 1. The three columns consist of ℓ, Fo (x10) and Fc (x10) on an absolute scale.

L	FO	FC
0 0 L		
4	424	433
8	779	650
12	114	117
14	73	78
16	120	125
18	0	30
20	60	55
24	36	29
1 0 L		
0	0	5
2	1186	1082
4	56	53
6	170	180
8	86	76
10	442	438
12	52	39
16	62	53
18	67	76
20	10	16
22	93	102
24	36	23
2 0 L		
0	839	818
2	135	118
6	46	52
10	193	197
12	380	391
14	100	108
16	121	128
18	33	27
20	57	72
22	0	16
24	39	36
3 0 L		
0	0	2
2	175	174
4	108	113
6	168	162
8	119	121
10	155	158
12	166	168
14	301	298
16	65	65
18	76	65
20	13	9
22	90	93
4 0 L		
0	532	555
2	58	62
4	171	172
6	17	30
8	190	199
10	86	92
12	150	152
14	41	37
16	74	75
18	0	8
20	57	50
22	24	5
5 0 L		
0	0	14
2	316	325
4	30	22
6	110	108
8	12	18
10	155	150
12	16	7
14	73	77
16	28	23
18	32	42
20	0	7
6 0 L		
0	292	310
2	0	8
4	74	81
6	0	9
8	132	131
10	13	8
12	51	49
16	30	36
18	19	10
7 0 L		
0	0	5
2	64	71
4	15	9
6	66	64
8	29	13
10	40	40
12	0	7
14	71	63
16	20	13
8 0 L		
0	47	52
2	24	10
4	46	44
6	0	2
8	29	36
10	25	18
12	56	44
9 0 L		
0	0	0
2	21	20
4	20	8
6	30	25
8	11	6
0 1 L		
0	25	1
C	0	1
1	157	162
2	937	939
4	85	83
5	140	117
6	274	284
8	78	62
10	458	448
12	112	106
14	174	164
15	98	100
16	67	70
17	81	84
18	58	56
19	23	6
20	23	15
21	42	32
22	78	77
23	33	23
24	37	23
25	53	47
1 1 L		
0	1328	1262
1	187	176
2	18	5
3	214	200
5	132	117
6	34	34
8	444	425
10	32	21
11	57	56
13	108	103
14	62	51
15	157	161
16	101	94
17	35	20
18	24	19
19	30	25
20	55	56
21	22	10
22	21	23
23	44	43
24	29	32
2 1 L		
0	75	67
1	574	555
2	205	197
4	113	98
5	57	76
7	65	55
8	27	20
9	85	85
10	182	193
11	58	58
12	45	44
13	81	80
14	277	281
15	112	99
16	37	34
17	26	22
18	63	64
19	14	7
20	26	11
21	35	28
22	86	92
23	27	7
24	21	16
3 1 L		
0	276	271
2	80	87
3	352	340
4	326	333
5	150	154
6	58	58
7	67	66
8	186	192
9	60	54
10	59	64
11	178	177
12	267	271
13	77	77
14	39	39
15	34	37
16	87	92
17	26	19
18	14	8
19	11	22
20	65	66
21	26	12
22	C	9
4 1 L		
0	40	37
1	175	183
2	187	187
3	31	29
4	39	41
5	47	47
6	149	143
7	11	24
8	15	12
9	30	24
10	124	121
11	32	37
12	15	21
13	40	46
14	136	130
15	40	44
16	15	12
17	28	27
18	50	46
19	17	3
20	0	5
22	53	54
5 1 L		
0	334	363
1	76	73
2	0	4
3	37	42
4	111	107
5	17	13
6	0	10
7	29	36
8	160	171
9	0	2
10	0	6
11	22	22
12	60	57
13	28	26
14	32	33
15	69	68
16	39	42
17	0	9
18	14	12
19	10	14
20	18	30
21	13	5
6 1 L		
0	11	12
1	27	31
2	117	122
3	35	37
4	0	9
5	11	12
6	95	93
7	21	12
8	0	10
9	24	21
10	78	76
11	0	15
12	20	19
13	40	33
14	66	62
15	29	25
16	27	22
17	28	24
18	21	21
19	0	2
7 1 L		
0	77	85
1	8	15
2	17	6
3	36	30
4	61	59
5	0	5
6	0	2
7	20	14
8	62	65
9	13	2
10	11	7
11	15	14
12	65	55
13	17	15
14	0	5
15	10	15
16	25	25
8 1 L		
0	15	3
1	31	27
2	22	23
3	0	4
4	0	10
5	0	13
6	40	40
7	0	5
8	12	5
9	16	12
10	18	18
11	0	6
12	0	7
13	20	11
9 1 L		
0	29	32
1	0	3
2	10	5
3	0	15
4	0	18
5	0	2
6	0	2
7	17	3
0 2 L		
0	150	172
1	649	617
2	207	199
3	113	105
4	365	357
6	172	176
7	75	69
8	305	292
9	101	103
10	78	81
11	70	72
12	158	168
13	62	68
14	96	100
15	212	222
16	86	72
17	30	22
18	30	28
19	49	41
20	53	45
21	30	26
22	24	16
23	76	69
24	35	34
1 2 L		
0	24	17
1	158	148
2	165	144
4	115	113
5	179	162
6	279	285
7	77	73
8	55	65
9	46	54
10	140	134
11	134	141
12	111	118
13	110	106
14	143	147
15	83	91
16	40	47
17	56	61
18	45	40
19	22	21
20	15	12
21	30	31
22	45	48
23	26	30
24	0	3
2 2 L		
0	99	84
1	119	116
2	50	50
3	357	344
5	105	105
6	90	84
7	130	128
8	187	186
9	41	45
10	106	98
11	281	285
12	188	178
13	61	59
14	48	59
15	66	60
16	69	73
17	21	22
18	6	3
19	32	39
20	62	64
21	22	19
22	0	16
23	20	23
3 2 L		
0	111	113
1	346	367
2	43	63
3	9	11
4	66	65
5	114	115
6	164	149
7	63	69
8	81	80
9	172	176
10	83	86
11	60	61
12	82	82
13	144	138
14	101	103
15	59	57
16	17	24
17	22	19
18	52	52
19	22	15
20	16	17
21	39	35
22	44	48
23	13	13
4 2 L		
0	144	154
1	95	101
2	34	28
3	130	128
4	101	106
5	48	45
6	25	20
7	55	67
8	123	131
9	38	42
10	49	45
11	123	122
12	82	79
13	29	29
14	48	47
15	63	69
16	30	44
17	9	5
18	7	12
19	23	32
20	48	41
21	13	12
22	13	10
5 2 L		
0	11	12
1	53	54
2	61	61
3	111	117
4	20	36
5	29	39
6	108	113
7	56	46
8	15	23
9	22	15
11	70	65
12	47	40
13	53	52
14	62	59
15	27	27
16	16	25
17	46	41
18	15	15
19	13	9
20	13	2
6 2 L		
0	45	46
1	76	81
2	18	17
3	6	17
4	75	72
5	27	22
6	31	21
7	40	37
8	81	74
9	40	33
10	15	11
11	31	20
12	61	55
13	17	13
14	26	17
15	53	47
16	39	27
17	0	15
18	11	7
7 2 L		
0	0	5
1	37	31
2	24	21
3	15	18
4	6	4
5	16	22
6	56	51
7	36	18
8	22	5
9	18	25
10	29	24
11	16	17
12	27	10
13	22	17
14	51	36
15	13	21
16	0	5
8 2 L		
0	31	29
1	0	5
2	0	5
3	46	35
4	20	20
5	0	10
6	10	7
7	26	12
8	17	26
9	13	7
10	11	4
11	42	33
12	34	20
9 2 L		
0	0	6
1	11	12
2	0	15
3	13	10
4	21	3
5	21	11
6	11	16
0 3 L		
0	67	67
1	159	160
2	102	112
3	351	350
4	211	201
5	114	121
6	146	161
7	153	157
8	122	122
9	54	54
10	123	129
12	15	37
13	80	84
14	90	85
15	59	58
16	19	16
17	57	54
18	30	21
19	41	34
20	19	8
21	31	27
22	34	17
23	41	28
1 3 L		
0	67	73
1	335	343
2	110	124
3	79	73
4	57	62
5	97	104
6	93	96
7	86	90
8	68	75
9	171	177
10	23	11
11	170	183
12	89	91
13	72	73
14	10	10
15	79	80
16	54	57
17	40	36
18	6	6
19	44	52
20	42	45
21	7	22
22	21	9
23	26	38
2 3 L		
0	59	56
1	194	187
3	200	216
4	24	30
5	125	126
6	84	78
7	100	98
8	34	36
9	155	153
10	46	45
11	126	131
12	57	64
13	126	121
14	36	30
15	41	40
16	11	16
17	28	29
18	38	42
19	25	20
20	18	25
21	31	29
22	0	16
23	30	27
3 3 L		
0	158	168
1	161	163
2	23	40
3	203	195
4	88	82
5	123	121
6	0	12
7	100	95
8	72	72
9	68	76
10	78	79
12	0	14
13	39	34
14	33	32
15	37	42
16	43	43
17	24	11
18	0	5
19	51	47
20	48	40
21	30	16
22	26	17
4 3 L		
0	21	15
1	76	74
2	75	75
3	174	181
4	49	49
5	62	68
6	67	63
7	76	77
8	20	19
9	68	65
10	16	21
11	101	103
12	35	32
13	58	57
14	24	26
15	11	16
16	0	13
17	40	37
18	12	18
19	0	10
20	17	10
21	19	19
5 3 L		
0	0	4
1	136	136
2	48	45
3	16	19
4	41	39
5	59	53
6	46	46
7	45	49
8	38	35
9	82	84
10	26	11
11	50	54
12	47	46
13	28	30
14	24	4
15	51	51
16	12	28
17	25	20
18	0	4
19	26	27
6 3 L		
0	6	10
2	15	20
3	65	60
4	33	21
5	27	34
6	38	40
7	43	42
8	15	19
9	34	32
10	30	25
11	61	52
12	0	9
13	31	23
14	35	31
15	21	23
16	0	5
17	25	17
7 3 L		
0	18	16
1	21	22
2	19	3
3	37	39
4	0	11
5	24	19
6	0	3
7	28	21
8	20	14
9	20	25
10	16	4
11	55	45
12	0	16
13	19	9
14	0	3
8 3 L		
0	24	7
1	15	19
2	23	22
3	20	23
4	0	3
5	28	22
6	0	11
7	7	13
8	11	5
9	20	20
10	0	4
0 4 L		
0	80	84
1	161	141
2	44	39
3	131	129
4	39	45
5	73	64
6	46	29
7	80	63
8	39	25
9	185	189
10	57	52
11	123	122
12	53	48
13	75	78
14	74	65
15	59	49
16	40	36
17	79	73
18	18	10
19	55	60
20	25	32
21	31	18
22	16	16
1 4 L		
0	0	13
1	103	115
2	79	89
3	163	166
4	15	29
5	133	146
6	33	38
7	81	90
8	32	35
9	70	69
10	69	68
11	138	139
12	31	38
13	60	65
14	27	12
15	58	61
16	22	29
17	36	43
18	0	9
19	42	35
20	0	5
21	29	21
22	16	2
2 4 L		
0	125	131
1	153	151
2	27	23
3	193	194
4	120	124
5	121	129
6	10	9
7	103	105
8	31	37
9	71	72
10	35	35
11	110	110
12	53	54
13	41	41
14	15	22
16	20	14
17	35	33
18	10	11
19	45	51
20	23	19
21	23	12
3 4 L		
0	24	20
1	114	116
2	157	155
3	196	192
4	17	31
5	144	147
6	27	32
7	72	65
8	28	27
9	48	44
10	31	27
11	78	70
12	20	10
13	47	46
14	28	33
15	27	25
16	29	6
17	37	39
18	0	4
19	0	7
20	20	11
4 4 L		
0	46	33
1	121	114
2	42	35
3	87	84
4	28	35
5	80	72
6	44	35
7	73	61
8	31	22
9	79	73
10	19	18
11	60	57
12	0	13
13	45	30
14	23	16
15	55	41
16	23	17
17	28	28
18	0	3
19	46	36
5 4 L		
0	11	10
1	26	40
2	11	4
3	73	65
4	13	19
5	57	54
6	21	19
7	53	50
8	29	22
9	24	33
10	26	29
11	67	63
12	25	18
13	24	28
14	0	15
15	30	29
16	14	12
17	11	24
6 4 L		
0	17	7
1	33	24
2	14	6
3	50	48
4	0	4
5	10	17
6	10	3
7	22	20
8	0	7
9	45	45
10	0	4
11	44	44
12	0	13
13	16	18
14	20	17
15	11	11
7 4 L		
0	0	5
1	29	27
2	31	22
3	28	28
4	23	6
5	42	35
6	11	2
7	15	12
8	22	7
9	24	20
10	0	6
11	18	20
12	0	1
8 4 L		
0	35	21
1	27	17
2	0	5
3	29	24
4	7	13
5	22	19
6	70	3
7	0	11
0 5 L		
1	108	101
2	41	46
3	27	38
4	76	75
5	91	108
6	32	24
7	63	66
8	35	43
9	75	76
10	45	42
11	71	63
12	26	23
13	46	41
14	19	11
15	53	57
16	21	16
17	45	39
18	27	24
19	32	33
20	18	8
1 5 L		
0	45	31
1	35	35
2	41	42
3	123	128
4	46	45
5	46	52
6	38	49
7	44	43
8	0	16
9	55	57
10	0	14
11	56	62
12	22	39
13	26	42
14	23	26
15	22	31
16	24	24
17	52	48
18	13	11
19	35	40
20	11	13
2 5 L		
0	41	32
1	86	88
2	59	60
3	97	98
4	31	17
5	118	121
6	35	36
7	40	35
8	0	10
9	39	35
10	42	42
11	29	35
12	0	9
13	20	29
14	33	27
15	21	33
16	11	8
17	40	35
18	0	22
19	11	14
3 5 L		
0	29	8
1	56	65
2	23	17
3	87	85
4	44	38
5	68	68
6	13	12
7	55	60
9	26	32
10	0	1
11	29	24
12	41	43
14	13	9
15	34	36
16	17	21
17	32	26
18	0	9
4 5 L		
0	6	6
1	38	47
2	16	22
3	47	50
4	0	5
5	64	63
6	13	22
7	27	30
8	9	2
9	29	31
10	24	16
11	31	33
12	0	11
13	15	21
14	0	5
15	32	27
16	16	4
17	23	25
5 5 L		
0	40	31
1	30	13
2	7	8
3	45	47
4	0	14
5	0	14
6	30	17
7	21	17
8	21	11
9	37	36
10	22	5
11	48	34
12	0	6
13	25	18
14	20	13
15	11	12
6 5 L		
0	13	9
1	42	32
2	0	9
3	0	17
4	21	18
5	32	34
6	22	4
7	0	14
8	30	16
9	30	24
10	0	11
11	27	17
12	0	2
7 5 L		
0	25	7
1	0	9
2	0	8
3	39	28
4	0	15
5	24	19
6	11	6
7	11	9
8	0	4
0 6 L		
0	67	64
1	29	19
2	37	35
3	49	38
4	51	48
5	36	41
6	50	44
7	26	42
8	30	24
9	0	15
10	33	30
11	55	44
12	34	22
13	26	14
14	13	4
15	15	16
16	14	18
17	27	16
1 6 L		
0	24	24
1	32	32
2	50	49
3	28	27
4	20	24
5	32	32
6	21	23
7	28	31
8	26	32
9	58	59
10	27	22
11	0	12
12	20	5
13	0	18
14	19	14
15	25	12
16	8	13
17	14	24
2 6 L		
0	47	44
1	0	14
2	9	14
3	20	23
4	38	37
5	40	36
6	17	6
7	25	36
8	28	11
9	26	16
10	0	8
11	26	19
12	24	27
13	0	4
14	21	6
15	33	21
16	16	19
17	0	12
3 6 L		
0	0	5
1	7	17
2	44	36
3	28	26
4	16	14
5	31	31
6	10	9
7	16	19
8	18	3
9	21	36
10	25	19
11	0	12
12	24	6
13	0	15
14	11	9
15	22	9
4 6 L		
0	47	42
1	0	5
2	0	5
3	18	14
4	16	21
5	0	13
6	0	5
7	10	25
8	17	14
9	22	19
10	15	10
11	22	20
12	21	9
13	11	5
14	20	3
5 6 L		
0	17	7
1	18	18
2	30	21
3	13	11
4	0	14
5	17	12
6	11	11
7	26	13
8	26	19
9	35	29
10	0	12
11	20	8
6 6 L		
0	0	10
1	25	1
2	18	6
3	0	17
4	0	16
5	23	17
6	13	11
7	16	4
8	6	7
0 7 L		
0	10	6
1	0	7
2	31	33
3	22	18
4	19	12
5	32	5
6	45	42
7	7	15
8	32	22
9	34	29
10	25	21
11	0	6
12	0	7
13	8	7
14	0	16
1 7 L		
0	40	34
1	16	2
2	0	12
3	C	4
4	28	31
5	0	20
6	30	21
7	25	22
8	36	35
9	22	4
10	0	11
11	14	11
12	0	16
13	14	8
2 7 L		
0	C	1
1	13	3
2	25	27
3	0	12
4	7	25
5	10	11
6	7	30
7	C	7
8	11	15
9	31	21
10	21	20
11	0	11
12	0	2
13	0	7
3 7 L		
0	28	31
1	0	1
2	19	12
3	11	4
4	13	14
5	0	4
6	22	19
7	27	19
8	41	29
9	0	13
10	0	2
11	23	7
4 7 L		
0	0	1
1	17	3
2	13	18
3	19	6
4	16	7
5	0	4
6	24	22
7	C	6
8	0	8
9	0	17
5 7 L		
0	11	13
1	0	4
2	0	3
3	0	6
4	25	14
5	0	11
0 8 L		
0	18	16
1	0	2
2	27	11
3	C	11
4	25	19
5	11	13
6	28	14
7	11	6
8	18	21
1 8 L		
C	8	2
1	0	4
2	14	15
3	0	9
4	28	16
5	14	10
7	0	6
2 8 L		
0	14	17
1	0	1
2	0	9
3	8	5
4	20	12
5	0	5
6	18	13
3 8 L		
C	0	1
1	0	2
2	14	11

Table 1. Final positional and thermal parameters and their standard errors for $OP(OCH_2)_3CCH_3$. The anisotropic temperature factor is of the form $\beta_{11}h^2+^3\beta_{22}k^2 + \beta_{33}\ell^2 + 2\beta_{12}hk + 2\beta_{13}h\ell + 2\beta_{23}k\ell)]$

Atom	x/a	y/b	z/c	β_{11}	β_{22}	β_{33}	β_{12}	β_{13}	β_{23}
	Molecule 1								
O_1	0.0	0.1183 (.0017)	-0.0816 (.0005)	0.0608 (.0037)	0.0601 (.0043)	0.0029 (.0002)	0.0	0.0	0.0011 (.0008)
P	0.0	0.0598 (.0006)	0.0	0.0279 (.0007)	0.0383 (.0013)	0.0026 (.0001)	0.0	0.0	0.0010 (.0003)
O_2	0.0	0.2632 (.0011)	0.0566 (.0011)	0.0336 (.0004)	0.0272 (.0022)	0.0035 (.0021)	0.0 (.0002)	0.0	0.0027 (.0005)
O_3	0.1829 (.0009)	-0.0807 (.0011)	0.0253 (.0003)	0.0414 (.0020)	0.0528 (.0023)	0.0034 (.0002)	0.0097 (.0018)	0.0042 (.0004)	0.0010 (.0006)
C_1	0.0	0.2006 (.0018)	0.1341 (.0006)	0.0400 (.0036)	0.0249 (.0031)	0.0030 (.0003)	0.0	0.0	0.0012 (.0008)
C_2	.1858 (.0012)	-0.1473 (.0015)	0.1048 (.0004)	0.0340 (.0024)	0.0562 (.0036)	0.0032 (.0002)	0.0155 (.0023)	0.0020 (.0006)	0.0031 (.0007)
C_3	0.0	-0.0538 (.0019)	0.1430 (.0005)	0.0212 (.0021)	0.0352 (.0034)	0.0021 (.0002)	0.0	0.0	-0.0013 (.0008)
C_4	0.0	-0.1217 (.0021)	0.2280 (.0006)	0.0377 (.0034)	0.0527 (.0055)	0.0031 (.0003)	0.0	0.0	0.0050 (.0010)

Table 1. continued

Atom	x/a	y/b	z/c	β_{11}	β_{22}	β_{33}	β_{12}	β_{13}	β_{23}
	Molecule 2								
O	0.5	0.3946 (.0017)	0.1672 (.0004)	0.0451 (.0029)	0.0703 (.0046)	0.0023 (.0002)	0.0	0.0	-0.0003 (.0081)
P	0.5	0.4392 (.0006)	0.2466 (.0002)	0.0247 (.0007)	0.0396 (.0012)	0.0022 (.0001)	0.0	0.0	-0.0001 (.0003)
O_2	0.5	0.6960 (.0013)	0.2681 (.0004)	0.0414 (.0028)	0.0336 (.0025)	0.0041 (.0003)	0.0	0.0	-0.0042 (.0007)
O_3	0.3157 (.0010)	0.3443 (.0011)	0.2913 (.0003)	0.0369 (.0019)	0.0655 (.0029)	0.0043 (.0002)	-0.0232 (.0019)	0.0009 (.0005)	-0.0024 (.0006)
C_1	0.5	0.7475 (.0022)	0.3500 (.0006)	0.430 (.0041)	0.0401 (.0044)	0.0033 (.0003)	0.0	0.0	0.0014 (.0010)
C_2	0.3185 (.0011)	0.3868 (.0015)	0.3710 (.0004)	0.0302 (.0021)	0.0481 (.0033)	0.0036 (.0003)	-0.0172 (.0022)	0.0006 (.0006)	-0.0001 (.0007)
C_3	0.5	0.5230 (.0017)	0.3902 (.0006)	0.0239 (.0024)	0.0286 (.0032)	0.0037 (.0003)	0.0	0.0	0.0003 (.0008)
C_4	0.5	0.5726 (.0025)	0.4769 (.0005)	0.0336 (.0030)	0.0678 (.0059)	0.0022 (.0002)	0.0	0.0	-0.0051 (.0010)

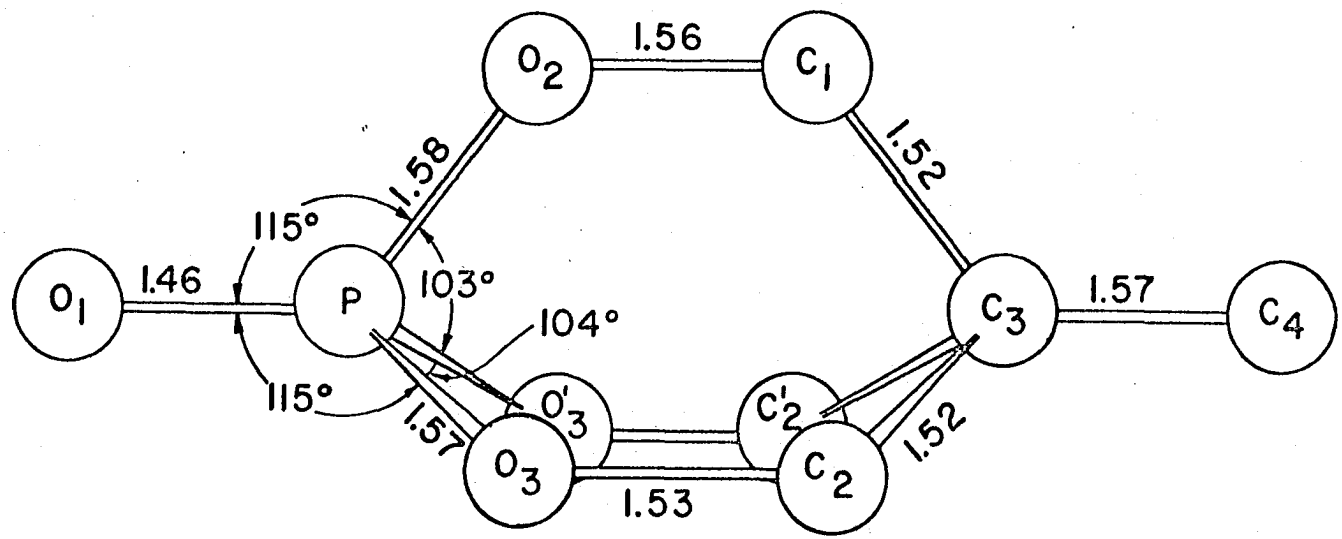

Figure 2. The molecular configuration of $OP(OCH_2)_3CCH_3$. The distances and angles are averages of the two crystallographically independent molecules of the asymmetric unit

distances and their standard errors as well as certain averages is given in Table 2. Table 3 contains a list of individual and averaged bond angles and their standard errors.

Large thermal parameters are common for most all of the atoms as might be expected from the soft crystal. The relatively large standard deviations as well as observed deviations in bond distances and angles reflect some of this thermal motion, but reflect, more so, the general quality of the data. The combination of decomposition, slight crystal shifting and inexperience (in perhaps the reverse order) in the data taking process led, it is felt, to the relatively large uncertainties in the finished product. More than one attempt was made to regrow fresh crystals of phos-oxide for the purpose of retaking the observed intensity data, but crystals of sufficient quality to warrant the project could not be found. The original crystal from which the intensity data was gathered was too badly decomposed to be used again.

The molecules of phos-oxide pack head to tail in a saw-tooth fashion on each mirror. A stereoscopic drawing of the molecules within the unit cell was computed in order to visualize the packing as well as the thermal motion of the atoms by means of OR TEP (21-22). The plotted result is given in Figure 3.

Table 2. Individual and averaged interatomic distances and their standard errors of $OP(OCH_2)_3CCH_3$

	Molecule 1		Molecule 2			
Atoms	Dist. (A)	Std. Error	Dist. (A)	Std. Error	Average Dist. (A)	Average Std. Error
$P-O_1$	1.491	0.017	1.436	0.015	1.464	0.016
$P-O_2$	1.575	0.016	1.577	0.018	1.574	0.015
$P-O_3$	1.556	0.012	1.578	0.012		
O_2-C_1	1.425	0.022	1.488	0.024	1.455	0.020
O_3-C_2	1.467	0.017	1.439	0.017		
C_1-C_3	1.524	0.028	0.516	0.030	1.519	0.024
C_2-C_3	1.528	0.018	1.506	0.018		
C_3-C_4	1.565	0.023	1.569	0.024	1.567	0.023
$P-C_3$	2.629	0.017	2.599	0.019	2.614	0.018

Table 3. Individual and averaged bond angles in degrees and their standard errors of $OP(OCH_2)_3CCH_3$

Atoms	Molecule 1		Molecule 2			
	Angle	Std. Error	Angle	Std. Error	Average Angle	Av. Std. Error
O_1-P-O_2	116.2	1.0	114.6	0.9	115.0	0.8
O_1-P-O_3	114.0	0.5	115.3	0.7		
O_2-P-O_3	103.3	0.6	103.1	0.6	103.7	0.6
O_3-P-O_3',[a]	104.7		103.8			
P-O_2-C_1	114.5	1.2	115.9	1.2	115.2	1.1
P-O_3-C_2	115.7	0.9	114.9	0.9		
O_2-C_1-C_3	111.1	1.4	106.1	1.8	108.7	1.4
O_3-C_2-C_3	108.5	1.2	109.2	1.2		
C_1-C_3-C_2	108.5	1.2	111.6	1.2	109.6	1.2
C_2-C_3-C_2'	109.9		108.5			
C_1-C_3-C_4	111.0	1.6	107.2	1.9	109.2	1.5
C_2-C_3-C_4	109.5		108.9	1.1		

[a] Primes refer to atoms related by the mirrors to the unprimed designation.

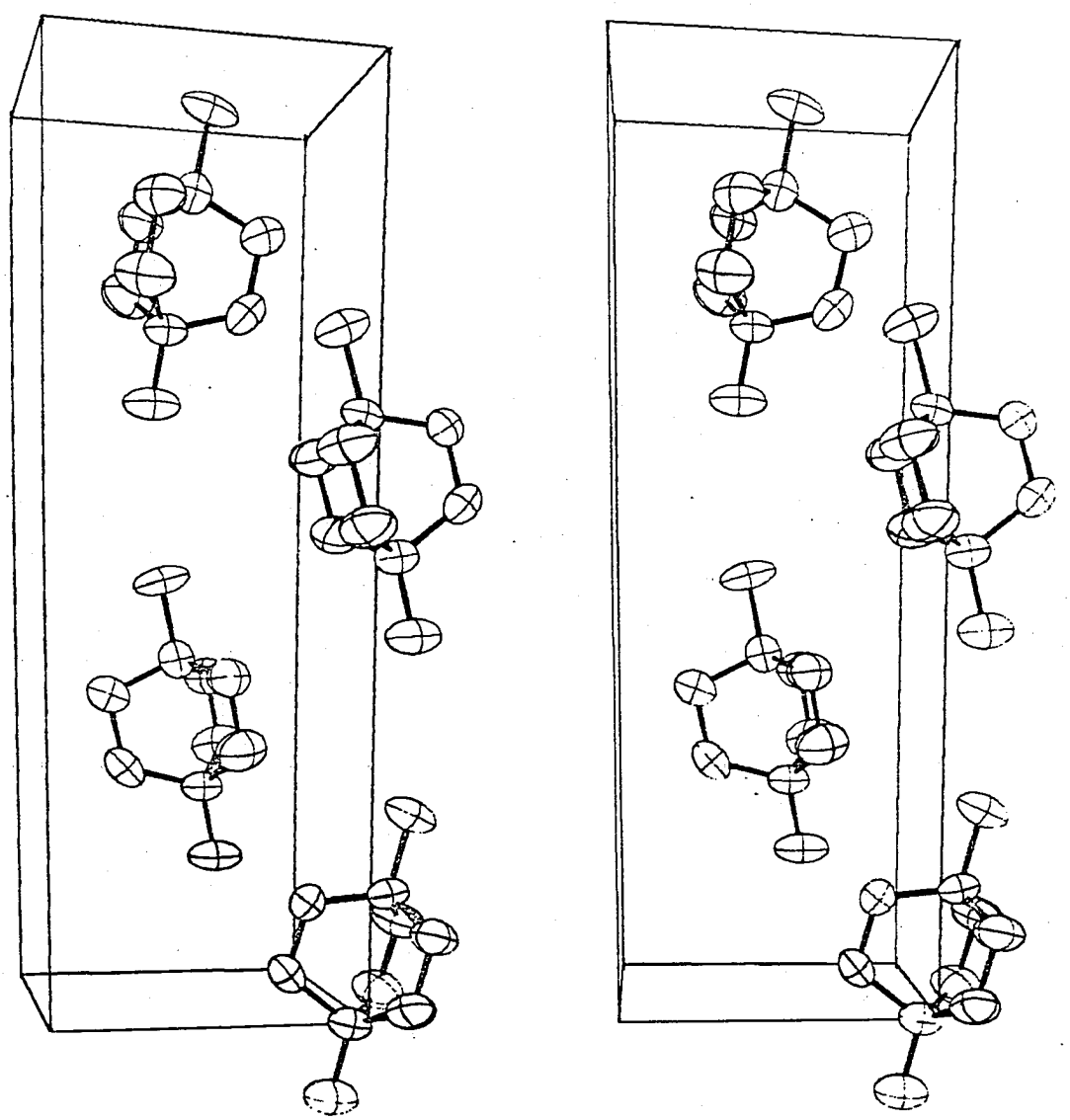

Figure 3. The atomic thermal ellipsoids (50 °/o probability) and the packing of the molecules of phos-oxide. The a axis runs horizontally to the left, and the c axis runs vertically upward

Discussion

The structure of phos-oxide clearly confirms the postulated molecular model. It thereby hopefully strengthens the use of IR and n.m.r. as structural tools in that the interpretation of their spectra was the basis of the molecular structure postulation.

The related bicyclic phosphate $OP(OCH_2)_3CC_2H_5$ has been reported by Neunhoeffer and Maiwald (23) to exist as dimers on the basis of their molecular weight determinations in benzene. Although this phenomena would not be entirely unexpected due to the large dipole moment, the molecules of phos-oxide in the crystal structure are clearly monomeric.

The dipole moment of phos-oxide has been observed to be 7.10 D (24). In the crystal the dipole moment vector of each molecule makes an angle of approximately 17° with the crystallographic c axis. Thus the component in the z direction is seen to be about 6.8 D. The electrical properties of crystalline electrets such as this have been discussed by Zhdanov (25). It would seem logical that, contrary to observation, such a high value of constant polarization would have an electric field observable in the formation of ice crystals on its surface.

The large dipole moment of the molecule probably accounts for the needle-like crystal habit. Whereas long, non-polar

molecules usually pack parallel to one another so as to form plate-like crystals, the dipole moment forces of a molecule such as this exert more of an influence on the packing than does the van der Waals forces.

The P^{31} n.m.r. spectra of the unoxidized bicyclic phosphite $P(OCH_2)_3CCH_3$ has been examined in terms of quantitative structural properties (7) by means of an empirical formula proposed by Parks (26) for estimating the X-P-X angle in PX_3 compounds. The formula relates the P^{31} chemical shift, referred to phosphoric acid under standard conditions, to a calculatable quantity D which is a measure of the "number of unbalanced p electrons" in the phosphorus valence shell. Its value is a function of the electronegativities of P and X and of another quantity β whose square is directly related to the X-P-X bond angle and whose expression has been derived by Coulson (27, pp. 193 ff.) as a function of the degree of hybridization in the system. The expressions for these quantities are in the literature (26, 28) and will not be presented here. At any rate they allow one to estimate X-P-X angles on the basis of assigned electronegativities and measured P^{31} chemical shifts. Such a treatment yielded a value of 104° for the OPO angle in $P(OCH_2)CCH_3$.

Although a correlation between P^{31} chemical shifts and PO_4 type compounds like phos-oxide has not been presented,

the constraints of the bicyclic structure make it probable that the bond angle changes within the cage would not be affected greatly in the oxidation of the phosphite to the phosphate. For example, the OPO angles of P_4O_6 and of P_4O_{10} differ by only 2.5° (29, 30, 31). In spite of expected similarity of the OPO bonding between phos and phos-oxide the calculated OPO angle of 104° seems amazingly, and surely to some extent accidentally, close to the observed values of 103.7 found in phos-oxide. The chief reservation with Park's expression is that the calculated value depends significantly on the assigned electronegativities. Nevertheless, this structure determination does add another point to the curve for correlating structural properties with n.m.r. results. Certainly there exists a need for methods which give cheaper and more rapid measurements of structural features than x-ray analysis.

The crystal structures of two other trialkyl phosphates have been recently reported, methyl pinacol phosphate, $OP(OC(CH_3)_2)_2(OCH_3)$ (32) and methyl ethylene phosphate, $OP(OCH_2)_2(OCH_3)$ (33).

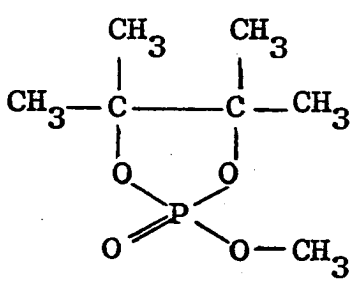

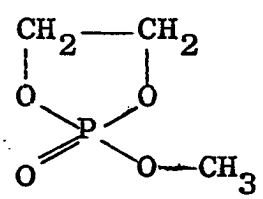

Since both of these compounds contain constrained five membered rings, the OPO and the POC angles are different from those found in phos-oxide. However, the 1.46 A P=O and the 1.57 A P-O bonds lengths found in phos-oxide agree within experimental error with the P=O and P-O distances reported in these two structures (1.44 and 1.57 A, respectively).

The OPO and POC angles found in phos-oxide (104 and 115°, respectively) as compared with those found in the above mentioned five membered ring compounds (99 and 112° respectively) indicate that less strain, as would be expected, is involved in this compound. On the other hand, the structure of an open chain dialkyl phosphate, dibenzyl phosphoric acid, $OP(OCH_2C_6H_6)_2$ (OH), has been reported by Dunitz and Rollett (34). Assuming the two ester groups in this structure represent a strainless system, it might be argued that the OPO and POC angles of this compound (104 and 120.5°, respectively) indicate that phos-oxide has some strain in the POC angles.

The parent caged phosphite, $P(OCH_2)_3CCH_3$, in a coordination compound in which four molecules of the phosphite are complexed with $AgClO_4$ has been studied by x-ray diffraction (35). The geometry is the same with the exception that the phosphorus bridgehead of the cage is more "pointed". The Ag-P-O angle is increased (from 115° (phos-oxide) to 118°), the OPO angle

is decreased (104° to 100°) and the POC angle has increased (115° to 122°).

The rare earth extractant properties of the related phosphate $OP(OCH_2)_3CC_5H_{11}$ (which is much less soluble in aqueous acid) have been studied by Goodman and Verkade (10). Tributyl phosphate has been previously shown to serve as a fairly good rare earth extractant. They found, however, that the extractant abilities of the caged phosphate were very poor and explained the phenomena on the basis of the strongly pi-bonded phosphoryl oxygen as evidenced by a very high P=O stretching frequency. They noted that the P=O stretching frequency of bicyclic phosphate was 1325 cm^{-1} as compared with 1260 cm^{-1} for the tributyl phosphate. Higher stretching frequencies are indicative of higher bond order which in turn might be thought of as withdrawal of electron density from the oxygen into the vacant d orbitals of the phosphorus, thereby explaining the decrease in extraction ability. The correlation between P=O stretching frequency and extractant ability has been noted also by Burger (36).

What is in question, however, is why the polycyclic phosphates have so much larger values for P=O stretching frequencies. It would be of interest to have accurate P=O distances at hand in order to construct a correlation table between stretching frequency and the P=O distance as has been done with carbonyl groups (37). Unfortunately, the only

three P=O distances known for trialkyl phosphate (all mentioned earlier) are within experimental error of one another.

In addition to the strong multiple bonding of terminal oxygen with the phosphorus some pi bonding between the ring oxygen and the phosphorus presumably exists as evidenced by the P-O bond lengths (1.57 A) which are significantly shorter than the sum of the covalent radii for phosphorus and oxygen (1.76 A) (38, p. 93). As the POC angle approaches 120°, indicative of sp^2 oxygen hybridization, the unhybridized lone pair p electrons become favorably positioned to donate to the vacant d orbitals on the phosphorus. The bond distances and angles involving phosphorus found in this compound have been correlated with several other sets in related phosphates and phosphites in Table 6 on page 67.

THE STRUCTURE OF ISOMER A

Introduction

Recently, Jenkins, Hutteman and Verkade reported the acid-catalyzed hydrolysis of the bicyclic phosphite 2,8,9-trioxa-1-phospha-adamantane, which yielded two isomeric products: isomer A (3-α-oxo-3-β-hydrido-7-β-hydroxyl-2,4-dioxa-3-phosphabicyclo[3.3.1]nonane) and isomer B (3-β-oxo-3-α-hydrido-7-β-hydroxy-2,4-dioxa-3-phosphabicyclo(3.3.1)-nonane) (39). The reaction is shown in Figure 4.

These two hydrolysates are among the few phosphorus acid diesters of the general type $OP(H)(OR)_2$ whose ligand properties with transition metals have been studied. Coordination of this type diester to the metal could take place through the oxygen (40), or it could take place directly through the phosphorus if the phosphoryl hydrogen were removed (41, 42, 43) or if the phosphoryl hydrogen migrated to the phosphoryl oxygen (44). In addition, coordination through the oxygen could take place even if the phosphoryl hydrogen was removed (45). Verkade and his co-workers reported that isomer A took the path whereby the phosphoryl hydrogen migrated to the phosphoryl oxygen in its coordination through the phosphorus with several transition metal salts. Evidence for this type of coordination was given by infrared studies which indicated

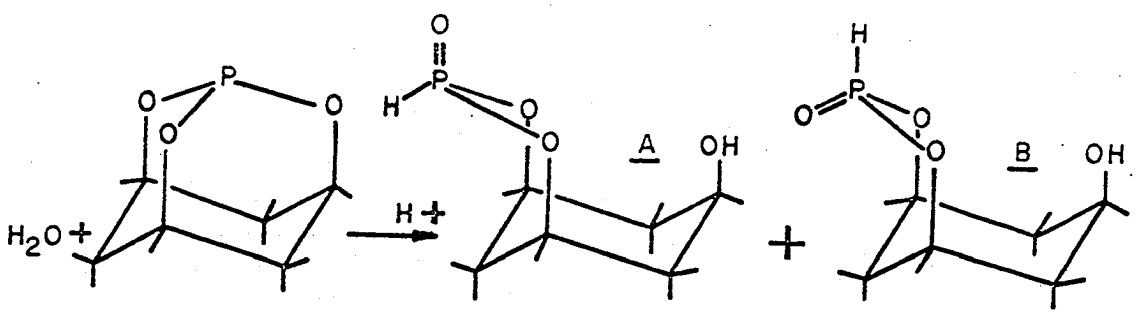

Figure 4. The acid-catalyzed hydrolysis of isomer A

a disappearance of the PH stretching mode upon complexation as well as the appearance of a new OH band.

The same study pointed out that in no case were metal complexes formed with isomer B. Modes and conditions for dehydration of the isomers back to the parent phosphite were also studied. Rationalization of these and other chemical and physical properties rely heavily on the postulated conformation and configuration of the two isomers.

Nuclear magnetic resonance and infrared absorption experiments have been used as tools for the postulation of the configuration and conformations of the two isomers. In their report (39) Verkade and his co-workers discussed the interpretation of these experiments. The proton n.m.r. spectra of isomer A is nearly identical to that of isomer B. The only major difference is that, whereas isomer A exhibits a PH doublet of single lines, isomer B exhibits a pair of 1331 quartets. It has been previously argued from geometrical factors that the presence of long range H^1-H^1 coupling could take place over five bonds (J_{HPOCCH} in this case) only if the bonds to the hydrogens were opposing and colinear (46). In this case the axial proton (down) of the methylene group directly below phosphorus could exhibit coupling with the phosphoryl hydrogen if the PH bond was colinear and opposed (up). The only conformation which would allow such a geometry is that shown for isomer B

in Figure 4. The more complicated splitting pattern of the PH hydrogen may then be explained by the additional coupling of the phosphoryl proton with each of the two methinyl protons and with the axial methylene proton directly below the phosphorus giving a pair of doublets of triplets which would appear as two 1331 quartets. Moreover, such a geometry might be expected to place the terminal oxygen in a position to hydrogen bond with equatorial hydrogen of the same methylene group. Hydrogen bonding has been known to influence the P=O stretching frequencies by 50-80 cm^{-1} when it has been to OH and NH groups (47). For isomer B it was found that, indeed, the P=O stretching frequency was lower than that for isomer A by an amount of 33 cm^{-1} (1241 and 1208 cm^{-1} respectively) lending support to the structure postulation. The P-H frequency also differs between isomers A and B implying an environmental change for the proton.

On the other hand the alcoholic OH stretching frequencies are the same (3450 cm^{-1}) for both isomers. The OH was thought to be axial on the basis of H-H coupling studies with n.m.r. An earlier, thorough study of an Arbuzov type ring cleavage of the same parent phosphite with RX conclusively showed from IR and n.m.r. arguments that X went onto the ring in the equatorial position (48, 49). The n.m.r. coupling of the axial proton of the carbon to which X was attached with the axial proton (<u>trans</u> to the first) of the adjacent carbon

was identified and measured. This same trans vicinal H-H coupling was found not to be present in the hydrolysates of the phosphite as would be expected if the OH occupied the equatorial position.

In summary, the lack of n.m.r. trans vicinal coupling - for either isomer indicates the axial site is occupied by the OH, and the constancy of the OH infrared stretching frequency for the two isomers supports the idea that the isomerism is not at the alcoholic group. That the isomerism takes place on the phosphoryl group is supported by the differences in stretching frequencies between the isomers for the P=O and the P-H bonds. That its form is as shown in Figure 4 is then evidenced by the long range H-H coupling for isomer B but not A and by the lowering of the P=O stretching frequency due to proposed hydrogen bonding in isomer B. Confirmation of the postulated conformation and configuration was one of the reasons for undertaking the x-ray structure of one of the isomers.

Additional interest in the crystal structure analysis stems from the fact there is little structural information concerning the stereochemical course of nucleophilic reactions of phosphites. Such knowledge would be expected to be particularly fruitful in the study of the stereochemistry of the reactions of polycyclic phosphites because, since the bond cleavage reactions do not fragment the molecule,

configurational and conformation analyses of the products of the reaction can be used to deduce the stereochemical aspects of the reaction (9). One problem in particular that might be raised is the question of the mechanism of the hydrolysis reaction of the parent phosphite as contrasted with the Arbuzov mechanism for its reaction with alkyl halides and halogens.

Experimental

Hydrolysis of 2,6,7-trioxa-1-phospha-adamantane is accomplished with the addition of a drop of perchloric acid to an acetone solution of equimolar quantities of the phosphite and H_2O. Separation of the two resulting isomers can be obtained by fractional crystallization from absolute ethanol (50). Dr. J. M. Jenkins kindly supplied crystals of isomer A using this procedure.

Single crystals suitable for x-ray analysis were grown from acetone by allowing the acetone to slowly evaporate from the solution. Several single crystals were selected from the batch and glued onto the ends of glass fibers with Duco cement. Both the film data and the intensity data were taken from crystals mounted in this manner. No protection from the atmosphere was found necessary. The crystal orientation was found in each case on an equi-inclination Weissenberg camera with CuKα radiation.

The Weissenberg camera with CuKα radiation was also used to gather h k 0 through h k 4 film data from one crystal and 0 k ℓ through 3 k ℓ data from another crystal. The observed diffraction symmetry from the films was m m m (orthorhombic). Systematic extinctions were found for h 0 0, $h \neq 2n$; 0 k 0, $k \neq 2n$; and 0 0 ℓ, $\ell \neq 2n$, which dictated uniquely the assignment of space group $P2_12_12_1$.

The lattice parameters were also obtained from Weissenberg photographs with CuKα radiation. Each photograph was individually calibrated by superimposing an aluminum powder diffraction pattern onto the film. After each photograph was taken and before the film was removed from its holder, the crystal was replaced with an aluminum powder sample. The x-ray port was then reopened and powder lines were recorded on the same film. The Weissenberg layer line screen was employed to limit the powder circles to 2 millimeter portions. The film holder was positioned in three places such that the film was calibrated in the middle region and on the two edges. $K\alpha_1$ spots were distinguishable from $K\alpha_2$ spots for both the aluminum powder pattern and for the single crystal of isomer A. Three different crystals were used to gather the data; two were mounted about the c axis and one about the a axis. The Bragg angles were carefully measured and calibrated. The lattice parameters and their standard deviations were obtained by a least-

squares treatment of the data (12) which employed a Nelson-Riley error function (51). The results are as follows:

$$a = 5.836 \pm 0.012 \text{ A}$$

$$b = 11.671 \pm 0.010 \text{ A}$$

$$c = 10.908 \pm 0.020 \text{ A}.$$

It is not understood why the method did not yield more accurate lattice constants than it did.

An unsuccessful attempt was made to obtain accurate lattice parameters from a powder sample with a Guinier focusing camera with CuKα radiation. Westman and Magnéli (52 - 53) have reported that accurate lattice parameters can be obtained by a simple and rapid procedure with such a camera. They reported parameters for an orthorhombic structure accurate to ± 0.03 °/o. Whereas it is felt by this author that such accuracies for routine structure determinations are not that important, the need for a simple rapid procedure yielding reliable results does exist. Furthermore, since there is a Guinier focusing camera in the Ames Laboratory, it was decided to investigate this method.

Single crystals were finely ground and mixed with varying amounts of standard KCl. The lattice parameters of KCl are very well known, and the presence of it in the sample yields powder lines which can be used to calibrate the rest of the lines. Before the film was developed, an arbitrary

scale, for later measurement of the relative positions of the powder lines, was printed on the edge of the film.

Unfortunately, the powder lines of isomer A turned out to be rather diffuse; the $K\alpha_1$, α_2 doublet could not be resolved. It was felt that perhaps the soft crystals of isomer A became stressed during the grinding process. A new batch was therefore ground in a liquid nitrogen bath. No marked improvements resulted in the powder patterns, however, and the project was abandoned.

The calculated density for four molecules per unit cell is 1.59 gms/cm^3. All atoms reside in general positions with one molecule per asymmetric unit. The structure determination therefore involves the determination of three positional parameters as well as the thermal parameters for eleven atoms excluding hydrogens.

A full octant of x-ray diffraction data was gathered at room temperature from a fresh crystal of dimensions 0.2 x 0.2 x 0.3 mm in the shape of an approximate parallelepiped with zirconium filtered molybdenum radiation. A General Electric XRD-5 x-ray unit equipped with a single crystal orienter and a scintillation counter was used to measure the intensities.

Before the commencement of the data gathering, the settings of the adjustments of the counting chain electronics were checked, the size of the diffracted beam aperture was

determined, the take-off angle was selected, and the crystal was examined for twinning. A brief description of the criteria used for determining these parameters follows.

The counting chain consists of an adjustable high voltage d.c. power supply to the scintillation counter. The preamplified output of the photoelectric cell of the counter is sent to an amplifier. The amplifier has a pulse height discriminating capability by means of two adjustable controls. An adjustable threshold voltage cuts out pulses of energy less than its setting. An adjustable "window" voltage control cuts out pulses of energy greater than the sum of the threshold and the window voltages. The intermediate pulses are admitted to the scaler and ratemeter.

The 0, 0, 6 reflection, which gave a counting rate of approximately 1200 counts per second, was chosen for obtaining the data for the electronic settings. A plot of the counting rate as a function of the d.c. high voltage supply to the scintillation counter for a fixed threshold voltage with the window at a maximum value displays a plateau between the lower voltages where diffracted beam quanta are lost and the higher voltages where noise gets mixed in with the true signal. The proper high voltage setting is the center of the plateau. A profile of the Kα peak (the distribution of energies of its pulses) is desired next so that the threshold may be set below the minimum energy of the Kα pulses and the

window may be set to extend the opening through the peak to the maximum energy of the pulses. Such a profile may be obtained for the previously chosen high voltage setting by using a very small window and plotting the counting rate as a function of the threshold. The threshold and window may then be set to include any desired percentage of the Kα peak. Since the width and position of the high voltage plateau is a function of the threshold, a recheck of the high voltage may be necessary if the chosen threshold is different from that used for the original high voltage selection.

A plot of the counting rate of a strong reflection as a function of the area of the aperture opening reveals, in essence, the size of the diffracted beam. The aperture size is chosen as small as possible but adequately large to allow the passage of the entire diffracted beam.

Pairs of reflections with similar chi and theta values may overlap in a normal theta scan if the take-off angle is too large. This is particularly troublesome with a fairly dense reciprocal lattice. One can, however, examine the calculated angles of the reflections for potentially troublesome reflections and scan them prior to taking data. Reduction of the take-off angle reduces the width of the peaks and the consequent overlap. The approximation of the scan measurement to the integrated intensity is in general better with the higher take-off angles, though.

By examining strip chart recordings of chi and omega scans of two or three reflections for splitting, one can detect slightly misoriented crystal fragments. It is noted, however, that precise twinning in which the reciprocal lattice points are more separated could pass this test. It is therefore advisable to take a zone of film data on the crystal selected for intensity data gathering.

All reflections within a 2θ sphere of 55° were scanned using a 100 second, 3.33° -2θ moving-crystal-moving-counter scan technique (15) with a 3° take-off angle and a 1.8° aperture to the counter. In addition the same 2θ ranges for 160 reflections, including all within a 2θ sphere of 20°, were scanned with an omega offset of 1.8° for establishing tables to be used for background correction. These background intensity measurements were plotted as a function of 2θ. It was discovered that the background was a function of chi as well as 2θ; therefore, two tables of the background as a function of 2θ were made up, one for chi between 0 and 25° and one for chi between 25 and 90°. These tables were used exclusively for the background of all reflections for which 2θ was greater than 16°. The actual observed background was used for reflections with 2θ less than 14°, and an average of the two was used between 14 and 16°.

The strip chart recording of each reflection was judged as to whether the intensity was clearly above background,

questionably above or indistinguishable from background. This information was coded for each reflection, and was carried through the data reduction to the cards containing the observed structure factors used for the structure determination and refinement.

Three standard peaks (0, 0, 6; 0, 6, 0; and 3, 0, 2) were periodically measured throughout the data taking process to monitor decomposition and crystal shifting. A linear least-squares fit of the decrease in intensity with x-ray exposure time was computed. (Higher order polynomial approximations were also computed, but no significant improvement was made on the least-squares fit.) Of the total 78 measurements taken only six fell outside of ±1.0 °/o of the linear least-squares line indicating that the trends were statistically meaningful. The results were as follows:

0,0,6 (strongest reflection of the three):	5.7% decrease in intensity
0,6,0 :	11.5% decrease in intensity
3,0,2 (weakest reflection of the three) :	1.5% increase in intensity
average :	5.2% decrease in intensity

One would be hard pressed to predict the effect of decomposition on the rest of the reflections from these results. After the structure was determined, independent refinements of data with a 5 °/o decomposition correction and of data with no

decomposition correction were carried out. The uncorrected data gave better agreement than the corrected data. Although it would be expected that most decomposition from x-ray exposure would be compound specific, it might be worthwhile expending some effort in an attempt to establish a criteria of some sort for selecting reflections to monitor decomposition. It was seen that the ones selected for this compound were of little value in measuring the general decomposition.

In addition to correction for background the intensities were corrected for non-linearity in the counter with the expression

$$I_{corr} = \frac{I_{raw}}{1 - I_{raw} \times 10^{-7}}$$

which corrects for the dead time of the counter electronics; for Lorentz-polarization ($LP = \frac{1 + \cos^2 2\theta}{2 \sin 2\theta}$); and for non-characteristic radiation ("streak") by means of the method of Benson and Fitzwater*. No absorption correction was made due to the small linear absorption coefficient (3.36 cm^{-1}).

A standard deviation was calculated for the intensity of each reflection by means of the following expression:

$$\sigma_I^2 = TC + (0.03\ TC)^2 + (0.03\ Bg)^2 + (0.05\ St)^2$$

---

*J. E. Benson and D. R. Fitzwater, Ames, Iowa, Ames Laboratory, U.S. Atomic Energy Commission. Streak correction. Private Communcation. 1964.

where TC = total counts

Bg = background

St = streak correction

TC represents the square of the statistical counting uncertainty, and the last three terms of the expression represent estimates of non-statistical systematic errors in their values. The corresponding standard deviation for the observed structure was calculated with the following expression:

$$\sigma_F = \left(\frac{I + \sigma_I}{LP} \right)^{1/2} - Fobs$$

where I = corrected intensity

LP = Lorentz-polarization factor

Fobs = the observed structure factor = $\left(\frac{I}{LP} \right)^{1/2}$

The more straightforwardly derived expression,

$$\sigma_F = \frac{Fobs \cdot \sigma_I}{2I} ,$$

was not used because it becomes inapplicable when I approaches zero.

Solution of the Structure

A set of sharpened data was computed by means of a program of Granoff and Jacobson[*]. Subsequently, both a

---

[*]B. Granoff and R. A. Jacobson, Ames, Iowa, Ames Laboratory, U.S. Atomic Energy Commision. A data sharpening program. Private Communcation. 1964.

sharpened and an unsharpened Patterson map were computed. The three Harker planes (x=1/2, y=1/2 and z=1/2) corresponding to the three screw axes were examined for large peaks representing phosphorus-phosphorus vectors. These Harker planes contain the P-P, O-O, and C-C vectors plus a few interatomic vectors that accidentally fall on these special planes. The ratio of the size of the P-P peaks to the O-O peaks should equal the ratio of the square of the number of electrons in P to the square of the number of electrons in O; one should, therefore, expect to be able to distinguish the P-P vectors from the rest.

A peak considerably larger than the rest, was indeed found on each of the three Harker planes. Furthermore, a single location in electron density space could be found for a phosphorus which could account for all three of the large peaks, and its position was thus established.

Spheres of 1.5 A radius were contoured about each of the P-P peaks for locating the P-O vectors. In this manner an oxygen location which was consistant with all possible P-O vectors and O-O vectors on the Patterson was found. Several other potential oxygen positions were found, but none were completely consistant with all of the possible vector combinations. It is felt that peak overlap prevented exact establishment of their positions. The potential oxygen positions were rejected or established with alternating

least-squares position refinement and electron density computations. Subsequent Fourier synthesis in conjunction with the examination of a scale model of the postulated molecular structure suggested sites for the inclusion of the remainder of the atoms.

Refinement of the model was achieved by a least-squares minimization of the quantity $\Sigma w(|Fo|-|Fc|)^2$, where $w = \frac{1}{\sigma_F^2}$, on an IBM 360/50 computer by means of ORFLS least-squares program (54) which employed Hartree-Fock-Slater scattering factor tables (18). With the inclusion of the last of the atoms the reliability index or R factor

$$R = \frac{\Sigma|Fo-sqFc|}{\Sigma|Fo|}$$

dropped from 0.191 to 0.084 in two cycles indicating the structure was indeed solved. It is of interest to note that this R factor value was computed with more than ten reflections per variable with isotropic temperature factors (two of which were not even allowed to vary at this point).

All atoms were eventually given anisotropic thermal parameters. Positions for the nine cyclohexane hydrogen atoms were calculated, and the atoms were included but were not allowed to vary. The phosphoryl and hydroxyl hydrogens were located on a difference Fourier synthesis. Their positions were adjusted to conform with typical bond distances and were not varied. When it was discovered that the

hydroxyl hydrogen might be weakly bonded to the terminal oxygen of a neighboring molecule, its position was allowed to vary. However, the shifts and standard deviations for its position were not meaningful, and the atom was returned to its calculated position.

Independent refinements with the 706 clearly observed reflections and with the total 1007 reflections were carried out, but the parameters and their standard deviations refined to very nearly the same values. The unweighted R factor for the final positional and thermal parameters (listed in Table 4) for the 706 observed reflections is 0.063. The weighted R factor

$$R_{wt} = \frac{(\Sigma w(Fo-sqFc)^2)^{1/2}}{(\Sigma Fo^2)^{1/2}}$$

is 0.052. Unweighted and weighted values for all reflections are 0.110 and 0.065, respectively. A listing of the observed and calculated structure factors based upon Table 4 is given in Figure 5.

It may be seen in Figure 5 that the calculated structure factors for the unobserved reflections are all very small and are frequently in contrast with the corresponding "observed" structure factors. Perhaps these 300 unobserved intensities should have been included with the 160 omega offset backgrounds in establishing the background tables. However, a structure factor calculation in which all

Table 4. Final positional and thermal parameters and standard errors (in parentheses) for isomer A. The anisotropic temperature factor expression is

$$\exp[-(h^2\beta_{11} + k^2\beta_{22} + \ell^2\beta_{33} + 2hk\beta_{12} + 2h\beta_{13} + 2k\beta_{23})]$$

Atom	x/a	y/b	z/c	β_{11}	β_{22}	β_{33}	β_{12}	β_{13}	β_{23}
P	0.24464	0.14923	0.11400	0.02902	0.00417	0.00660	0.00184	-0.00044	-0.00058
	(0.00042)	(0.00014)	(0.00020)	(0.00062)	(0.00011)	(0.00014)	(0.00035)	(0.00038)	(0.00015)
O_1	0.03964	0.19142	0.16795	0.03904	0.00906	0.01147	0.00512	0.00083	-0.00356
	(0.00100)	(0.00042)	(0.00050)	(0.00223)	(0.00049)	(0.00060)	(0.00090)	(0.00097)	(0.00048)
O_2	0.20607	0.06706	0.00445	0.02985	0.00519	0.00685	0.00328	-0.00084	-0.00004
	(0.00080)	(0.00036)	(0.00040)	(0.00188)	(0.00032)	(0.00043)	(0.00073)	(0.00081)	(0.00034)
O_3	0.40957	0.08850	0.20432	0.03412	0.00584	0.00611	0.00060	-0.00183	-0.00131
	(0.00092)	(0.00037)	(0.00043)	(0.00183)	(0.00036)	(0.00042)	(0.00076)	(0.00087)	(0.00036)
O_4	0.09120	-0.12298	0.18251	0.02834	0.00647	0.01099	0.00097	0.00314	0.00183
	(0.00100)	(0.00042)	(0.00057)	(0.00180)	(0.00044)	(0.00063)	(0.00080)	(0.00104)	(0.00046)
C_1	0.38308	-0.01431	-0.03544	0.03147	0.00606	0.00447	0.00254	0.00132	-0.00045
	(0.00136)	(0.00055)	(0.00057)	(0.00272)	(0.00057)	(0.00055)	(0.00114)	(0.00111)	(0.00051)
C_2	0.30228	-0.13372	-0.00470	0.02769	0.00487	0.00577	0.00085	0.00053	-0.00132
	(0.00115)	(0.00051)	(0.00059)	(0.00277)	(0.00050)	(0.00056)	(0.00097)	(0.00100)	(0.00045)
C_3	0.30024	-0.16075	0.13328	0.02822	0.00481	0.00906	0.00173	0.00399	0.00242
	(0.00120)	(0.00056)	(0.00065)	(0.00291)	(0.00049)	(0.00085)	(0.00110)	(0.00124)	(0.00056)

Table 4. continued

Atom	x/a	y/b	z/c	β_{11}	β_{22}	β_{33}	β_{12}	β_{13}	β_{23}
C_4	0.50614	-0.11446	0.19934	0.02463	0.00554	0.00677	0.00303	-0.00056	0.00113
	(0.00119)	(0.00057)	(0.00073)	(0.00246)	(0.00055)	(0.00065)	(0.00099)	(0.00120)	(0.00056)
C_5	0.58175	0.00460	0.16191	0.01417	0.00653	0.00847	0.00283	-0.00322	-0.00046
	(0.00118)	(0.00061)	(0.00059)	(0.00198)	(0.00055)	(0.00072)	(0.00109)	(0.00109)	(0.00058)
C_6	0.60597	0.01370	0.02532	0.02305	0.00525	0.00896	-0.00079	0.00544	0.00059
	(0.00134)	(0.00054)	(0.00066)	(0.00244)	(0.00057)	(0.00075)	(0.00107)	(0.00126)	(0.00059)
H(P)	0.36607	0.23236	0.06841						
$H(O_4)$	0.07135	-0.18462	0.22544						
$H(C_1)$	0.40409	-0.01039	-0.12661						
$H(C_2)$	0.14261	-0.14546	-0.03625						
$H(C_3)$	0.31698	-0.24734	0.13566						
$H(C_4)$	0.46979	-0.11241	0.28968						
$H(C_4)$	0.63742	-0.16846	0.18607						
$H(C_5)$	0.73546	0.02002	0.20071						
$H(C_6)$	0.65353	0.09400	0.00307						

Figure 5. Comparison of calculated and observed structure factors for isomer A upon the parameters of Table 5. The three columns consist of k, F_o (x10) and F_c (x10). Negative values of F_o denote unobserved reflections

K	FO	FC
0	K	0
		1
		2
		3
		4
		5
		6
		7
		8
		9
		10
		11
		12
0	K	1
1	370	330
2	327	255
3	314	291
4	123	100
5	319	295
6	444	418
7	251	241
8	139	134
9	106	107
10	137	171
11	256	265
12	120	104
13	-81	41
14	161	144
0	K	2
1	221	220
2	692	660
3	1512	1508
4	602	615
5	-0	19
6	264	255
7	606	605
8	-37	32
9	126	112
10	239	248
11	63	95
12	-34	33
13	219	214
14	196	144
0	K	3
1	342	310
2	720	752
3	352	337
4	289	287
5	341	334
6	281	285
7	197	224
8	392	380
9	-0	66
10	242	235
11	-0	11
12	118	130
13	-30	1
14	-58	35
0	K	4
0	-145	75
1	1122	1091
2	998	976
3	361	340
4	286	310
5	169	153
6	683	696
7	-107	42
8	132	112
9	301	307
10	315	313
11	152	143
12	93	69
13	112	100
14	59	81
0	K	5
1	433	406
2	-94	82
3	-66	25
4	311	310
5	898	922
6	-73	23
7	146	148
8	-40	32
9	588	582
10	-78	58
11	-81	26
12	-77	64
13	180	159
0	K	6
0	1131	1107
1	-119	60
2	364	359
3	397	375
4	-62	34
5	383	392
6	-92	7
7	468	463
8	-51	84
9	270	266
10	177	148
11	229	195
12	-69	50
13	230	191
0	K	7

	1	-57 45
	2	296 297
	3	-80 48
	4	208 208
	5	64 95
	6	508 501
	7	-0 46
	8	213 175
	9	-23 11
	10	-45 65
	11	-76 41
	12	279 249
0	K	8
	0	274 266
	1	92 151
	2	-34 54
	3	183 165
	4	154 149
	5	222 218
	6	232 224
	7	-155 82
	8	-0 33
	9	-68 36
10	344	337
11	-66	27
12	-88	55
0	K	9
1	227	212
2	119	131
3	288	298
4	-0	68
5	112	106
6	-89	49
7	-13	18
8	-77	59
9	100	112
10	246	203
11	216	181
0	K	10
	0	409 422
	1	-35 51
	2	-0 21
3	186	151
4	411	418
5	-0	71
6	115	99
7	-65	52
8	-46	22
9	178	149
10	110	98
0	K	11
	1	-0 2
2	259	258
3	-0	18
4	-61	14
5	90	101
6	-95	88
7	159	120
8	160	165
9	63	79
0	K	12
	0	138 139
	1	147 128
	2	-80 21
	3	151 145
	4	76 80
	5	-82 57
	7	96 80
0	K	13
	1	109 91
	2	-0 53
	3	-75 15
	4	-27 40
	5	212 183
0	K	14
	0	-37 63
	1	-34 62
	2	-0 6
1	K	0
	1	17471688
	2	243 199
	3	16551668
	4	567 554
	5	494 494
	6	237 228
	7	391 384
	8	147 112
	9	346 352
10	-66	29
11	262	266
12	-44	11
13	269	261
14	138	79
1	K	1
	0	343 305
	1	833 802
	2	790 747

	3	653 640
	4	155 138
	5	303 300
	6	270 267
	7	277 302
	8	122 126
	9	183 188
10	224	254
11	159	178
12	297	301
13	105	80
14	-79	20
15	146	112
1	K	2
0	1279	1260
1	507	473
2	821	784
3	424	414
4	1054	1096
5	153	170
6	300	327
7	176	175
8	-64	87
9	150	176
10	404	413
11	93	109
12	-69	92
13	-95	87
14	138	136
1	K	3
0	336	310
1	429	441
2	349	349
3	365	361
4	398	402
5	562	577
6	302	307
7	168	167
8	165	181
9	303	312
10	159	182
11	131	136
12	-0	20
13	134	126
1	K	4
0	397	373
1	130	121
2	147	143
3	769	784
4	171	172
5	265	266
6	148	143
7	583	594
8	103	80
9	171	183
10	148	149
11	117	141
12	-0	44
13	153	156
1	K	5
0	138	132
1	354	349
2	446	453
3	256	265
4	512	527
5	198	172
6	460	479
7	60	75
8	432	434
9	155	188
10	275	273
11	-85	73
12	170	157
13	-64	62
1	K	6
0	995	589
1	253	243
2	171	166
3	186	187
4	247	234
5	244	258
6	548	573
7	192	178
8	163	177
9	-0	8
10	282	273
11	-50	57
12	109	67
13	-68	70
1	K	7
0	79	74
1	254	248
2	181	169
3	150	166
4	123	109
5	394	406
6	-74	117
7	206	213
8	88	80
9	241	246
10	-73	42
11	157	124
12	-89	72

1	K	8
0	354	367
1	320	322
2	180	179
3	348	335
4	119	120
5	-0	26
6	202	200
7	205	224
8	98	124
9	280	262
10	-89	18
11	185	166
12	114	80
1	K	9
0	145	127
1	-53	46
2	338	337
3	178	198
4	-0	55
5	85	78
6	133	122
7	-18	56
8	169	153
9	-95	65
10	74	72
1	K	10
0	164	156
1	249	241
2	100	100
3	180	183
4	211	189
5	126	136
6	91	92
7	-82	106
8	-2	56
9	-2	73
10	165	149
1	K	11
0	91	96
1	228	215
2	-47	40
3	128	154
4	108	106
5	-153	166
6	-157	139
7	-0	15
8	-0	38
9	109	110
1	K	12
0	80	101
1	-100	74
2	-58	54
3	-77	60
4	121	116
5	80	46
6	-2	51
7	142	108
1	K	13
0	47	90
1	57	72
2	125	128
3	-0	27
4	160	143
6	145	147
2	K	0
C	389	386
1	145	108
2	155	159
3	176	184
4	486	513
5	177	177
6	250	285
7	459	474
8	96	46
9	203	203
10	614	624
11	-74	27
12	120	101
13	-50	0
14	233	219
2	K	1
0	268	254
1	381	386
2	463	482
3	433	415
4	91	92
5	328	321
6	458	478
7	275	263
8	176	191
9	210	203
10	179	190
11	196	208
12	148	141
13	115	104
14	-90	95
2	K	2
C	1239	1220

1	459	464
2	214	208
3	905	888
4	615	598
5	104	134
6	238	234
7	436	440
8	119	138
9	338	358
10	0	34
11	191	212
12	-0	42
13	266	252
14	68	40
2	K	3
0	242	241
1	351	353
2	374	375
3	384	359
4	159	160
5	487	502
6	339	339
7	191	191
8	357	375
9	406	431
10	8	84
11	-26	80
12	225	234
13	103	98
14	134	75
2	K	4
0	248	258
1	518	515
2	495	483
3	410	399
4	447	456
5	135	126
6	487	489
7	-105	106
8	216	219
9	14	108
10	227	234
11	54	64
12	110	106
2	K	5
0	240	228
1	292	317
2	-0	36
3	164	170
4	113	117
5	451	466
6	207	227
7	145	165
8	-74	97
9	233	240
10	65	71
11	130	135
12	-97	88
2	K	6
0	225	223
1	444	470
2	384	376
3	541	553
4	78	80
5	171	193
6	376	395
7	344	376
8	94	115
9	136	97
10	-19	53
11	-89	98
12	-47	36
2	K	7
0	212	201
1	333	346
2	332	326
3	171	173
4	235	242
5	233	236
6	137	121
7	153	152
8	221	225
9	138	113
10	35	90
11	114	126
12	138	124
2	K	8
0	723	729
1	232	235
2	137	120
3	320	296
4	430	447
5	124	151
6	125	149
7	176	179
8	66	98
9	-59	67
10	190	175
2	K	9
0	172	119
1	291	298
2	-0	31

3	212	221
4	42	73
5	157	149
6	-0	31
7	82	97
8	-59	39
9	-82	88
2	K	10
0	179	183
1	197	185
2	-69	54
3	204	214
4	-76	55
5	-0	49
6	152	133
7	177	155
8	-0	38
9	-34	76
2	K	11
0	139	129
1	-0	32
2	235	240
3	-105	64
4	102	108
5	-0	59
6	111	119
7	2	68
8	61	99
2	K	12
0	-70	39
1	-45	46
2	117	89
3	-75	81
4	-2	3
5	-0	44
6	153	155
2	K	13
0	-73	42
1	166	164
2	102	80
3	K	0
1	275	283
2	81	69
3	124	96
4	101	109
5	183	197
6	-62	21
7	469	489
8	178	183
9	261	262
10	-0	27
11	128	132
12	172	165
13	285	262
3	K	1
0	75	65
1	156	166
2	461	469
3	151	151
4	167	164
5	459	462
6	163	150
7	180	193
8	336	348
9	327	347
10	-95	76
11	C	70
12	104	133
13	134	100
3	K	2
0	425	442
1	514	517
2	480	477
3	292	294
4	159	161
5	297	307
6	532	554
7	50	71
8	139	171
9	-58	61
10	256	257
11	98	121
12	172	152
13	-105	44
3	K	3
0	94	98
1	275	288
2	105	81
3	259	259
4	278	283
5	264	257
6	421	439
7	221	243
8	179	217
9	242	268
10	144	166
11	148	157
12	139	147
13	-59	57

3	K	4
0	662	633
1	280	268
2	-77	39
3	340	348
4	295	290
5	127	107
6	134	138
7	329	362
8	-0	28
9	112	143
10	-0	12
11	-0	60
12	-24	19
13	170	146
3	K	5
0	180	187
1	83	95
2	329	318
3	152	160
4	279	238
5	160	162
6	216	218
7	119	120
8	138	134
9	143	135
10	27	49
11	-39	41
12	123	126
3	K	6
0	468	472
1	177	189
2	172	186
3	359	369
4	496	508
5	88	103
6	54	88
7	61	57
8	-25	52
9	98	107
10	190	186
11	-94	83
12	79	85
3	K	7
0	-62	55
1	223	231
2	162	182
3	171	179
4	169	190
5	161	195
6	-0	47
7	143	159
8	-48	38
9	-111	89
10	-0	44
11	113	111
3	K	8
0	-0	76
1	358	366
2	380	394
3	314	335
4	233	231
5	106	113
6	40	89
7	183	183
8	-73	44
9	-81	77
10	141	145
3	K	9
0	-0	62
1	25	76
2	146	150
3	54	81
4	123	127
5	-0	34
6	-0	26
7	-75	69
8	91	121
9	-0	31
3	K	10
0	255	274
1	-70	77
2	-78	24
3	120	119
4	83	100
5	-62	68
6	162	165
7	-33	83
8	2	66
3	K	11
0	86	107
1	137	136
2	-61	28
3	-64	67
4	-0	69
5	141	150
6	-25	12
3	K	12
0	-71	93

	1	-66 67
	2	-33 55
	3	132 147
	4	2 53
4	K	0
	0	219 189
	1	296 312
	2	408 393
	3	471 483
	4	450 500
	5	132 122
	6	119 139
	7	159 169
	8	106 76
	9	-96 60
10	290	283
11	123	103
12	-87	3
4	K	1
0	141	147
1	288	256
2	208	203
3	174	136
4	290	269
5	298	302
6	243	243
7	144	140
8	239	239
9	100	93
10	-0	38
11	124	133
12	124	128
4	K	2
0	-53	4
1	185	176
2	246	249
3	400	413
4	230	229
5	-0	52
6	218	247
7	234	251
8	76	100
9	168	168
10	89	81
11	127	112
12	-83	54
4	K	3
0	308	325
1	151	172
2	297	297
3	-15	62
4	103	132
5	257	262
6	185	214
7	61	92
8	96	109
9	91	144
10	21	44
11	42	76
12	137	136
4	K	4
0	370	372
1	148	143
2	145	167
3	117	122
4	192	195
5	66	139
6	305	317
7	76	69
8	-63	85
9	30	95
10	133	137
11	-87	5
12	59	57
4	K	5
0	95	60
1	241	254
2	214	206
3	153	145
4	-48	69
5	216	219
6	138	166
7	-71	37
8	204	220
9	138	137
10	0	47
11	-59	56
4	K	6
0	121	113
1	191	194
2	-0	41
3	315	321
4	138	122
5	71	55
6	141	140
7	162	158
8	158	161
9	145	113
10	-0	39
11	99	85
4	K	7

	0	144 144
	1	134 144
	2	187 194
	3	190 102
	4	-0 43
	5	-57 76
	6	141 121
	7	-100 109
	8	217 184
	9	116 83
10	-38	71
4	K	6
	0	243 251
	1	85 112
	2	-0 48
	3	-73 77
	4	164 168
	5	-6 58
	6	-95 87
	7	162 144
	8	-46 44
	9	-0 32
4	K	9
	0	120 123
	1	82 86
	2	6 77
	3	-0 34
	4	-0 19
	5	109 112
	6	-28 81
	7	-47 42
	8	-0 74
4	K	10
	0	174 177
	1	90 107
	2	-0 41
	3	130 143
	4	-0 48
	5	-0 19
	6	76 110
	7	115 112
4	K	11
	0	-0 29
	1	-47 65
	2	-0 50
	3	-0 33
	4	123 87
4	K	12
	0	-0 8
	1	-0 52
5	K	0
	1	165 150
	2	538 533
	3	409 397
	4	78 100
	5	-42 42
	6	159 162
	7	124 105
	8	-71 39
	9	125 121
10	-62	57
11	-112	65
5	K	1
	0	-48 23
	1	283 272
	2	272 266
	3	295 286
	4	150 156
	5	191 181
	6	-79 59
	7	56 57
	8	112 121
	9	-70 43
10	-49	31
11	114	90
5	K	2
	0	327 322
	1	219 222
	2	153 148
	3	155 166
	4	216 227
	5	98 108
	6	197 191
	7	-31 31
	8	54 70
	9	-48 79
10	138	133
11	-85	32
5	K	3
	0	-0 31
	1	164 188
	2	103 130
	3	-18 38
	4	119 133
	5	147 177
	6	-0 32
	7	-0 46

	8	91 96
	9	95 107
10	-87	22
5	K	4
	0	-51 74
	1	170 191
	2	95 119
	3	264 267
	4	158 159
	5	74 94
	6	0 95
	7	174 188
	8	101 104
	9	123 79
10	0	17
5	K	5
	0	-73 32
	1	106 135
	2	128 118
	3	171 183
	4	143 148
	5	106 130
	6	85 101
	7	115 122
	8	157 156
	9	104 91
10	-88	59
5	K	6
	0	120 125
	1	88 63
	2	209 204
	3	158 119
	4	175 153
	5	113 88
	6	-112 91
	7	157 126
	8	-89 46
	9	-75 35
5	K	7
	0	-75 27
	1	-102 75
	2	92 106
	3	-122 100
	4	133 112
	5	-0 22
	6	95 30
	7	-57 19
	8	92 65
5	K	8
	0	-13 42
	1	-67 78
	2	-18 35
	3	105 82
	4	-73 63
	5	-33 25
	6	-30 62
	7	172 132
5	K	9
	0	-0 46
	1	-0 11
	2	119 119
	3	0 19
	4	-0 43
	5	-59 73
5	K	10
	0	-65 8
	1	-82 41
	2	74 84
	3	-89 13
	4	127 109
	5	101 77
6	K	0
	0	330 320
	1	170 175
	2	114 92
	3	93 73
	4	-73 21
	5	89 111
	6	142 158
	7	-44 21
	8	121 100
	9	-59 8
6	K	1
	0	0 25
	1	140 127
	2	164 156
	3	62 64
	4	-0 31
	5	132 107
	6	128 84
	7	-67 43
	8	91 70
	9	135 86
6	K	2
	0	-0 22
	1	195 184
	2	118 102
	3	95 97

	4	0 72
	5	-26 22
	6	81 54
	7	179 150
	8	-96 35
	9	-105 19
6	K	3
	0	-0 18
	1	59 93
	2	85 92
	3	-0 66
	4	108 100
	5	96 76
	6	-70 61
	7	-66 18
	8	145 134
6	K	4
	0	151 150
	1	-0 60
	2	-0 51
	3	96 100
	4	147 123
	5	-0 47
	6	95 95
	7	-88 44
	8	-98 59
6	K	5
	0	-0 36
	1	67 78
	2	-0 55
	3	92 61
	4	-43 61
	5	148 131
	6	-0 32
	7	88 62
6	K	6
	0	-0 7
	1	120 120
	2	-66 60
	3	130 130
	4	103 95
	5	149 129
	6	-96 30
	7	-82 35
	8	92 65
6	K	8
	0	-0 50
	1	68 51
	2	-0 21
	3	130 101
7	K	0
	1	-73 20
	2	-103 19
	3	134 111
	4	-83 31
	5	121 85
7	K	1
	0	-65 8
	1	-82 41
	2	74 84
	3	-89 13
	4	127 109
	5	101 77
7	K	2
	0	93 51
	1	-111 56
	2	134 109
	3	-85 30
	4	164 135
7	K	3
	0	-0 3
	1	106 84
	2	-41 28
	3	118 95
	4	-44 2
7	K	4
	0	-76 24
	1	-83 65
	2	90 58
	3	119 89
7	K	5
	0	-2 35
	1	-2 24
	2	126 90

unobserved reflections were given the value of zero yielded unweighted and weighted R-factors of 0.145 and 0.078, respectively.

Structure

The molecular structure of isomer A is shown in Figure 6. A stereoscopic drawing of the molecule excluding the cyclohexane hydrogens was computed with a plotting program of Johnson (21 - 22) in order to visualize the thermal motion of the atoms. The plotted result is given in Figure 7. Interatomic distances and angles and their standard deviations were computed on the basis of the complete variance-covariance matrix of the last least-squares cycle with ORFFE (20). The results are listed in Table 5.

A stereoscopic drawing was also computed and plotted for the molecule and its symmetrically related neighbors within the unit cell to demonstrate the packing of the molecules. This drawing is shown in Figure 8. From this drawing and the table of interatomic distances (Table 5) one would presume that the packing makes use of a weak hydrogen bond between the hydroxyl hydrogen and O_1 of the neighboring molecule related by the twofold screw axis in the y direction. The O_4-O_1' distance (2.816 ± 0.007 A) is with in the range of 0-0 systems which are designated as being hydrogen bonded (55). Moreover, the difference Fourier indicated that the hydroxyl hydrogen was between O_4 and O_1'

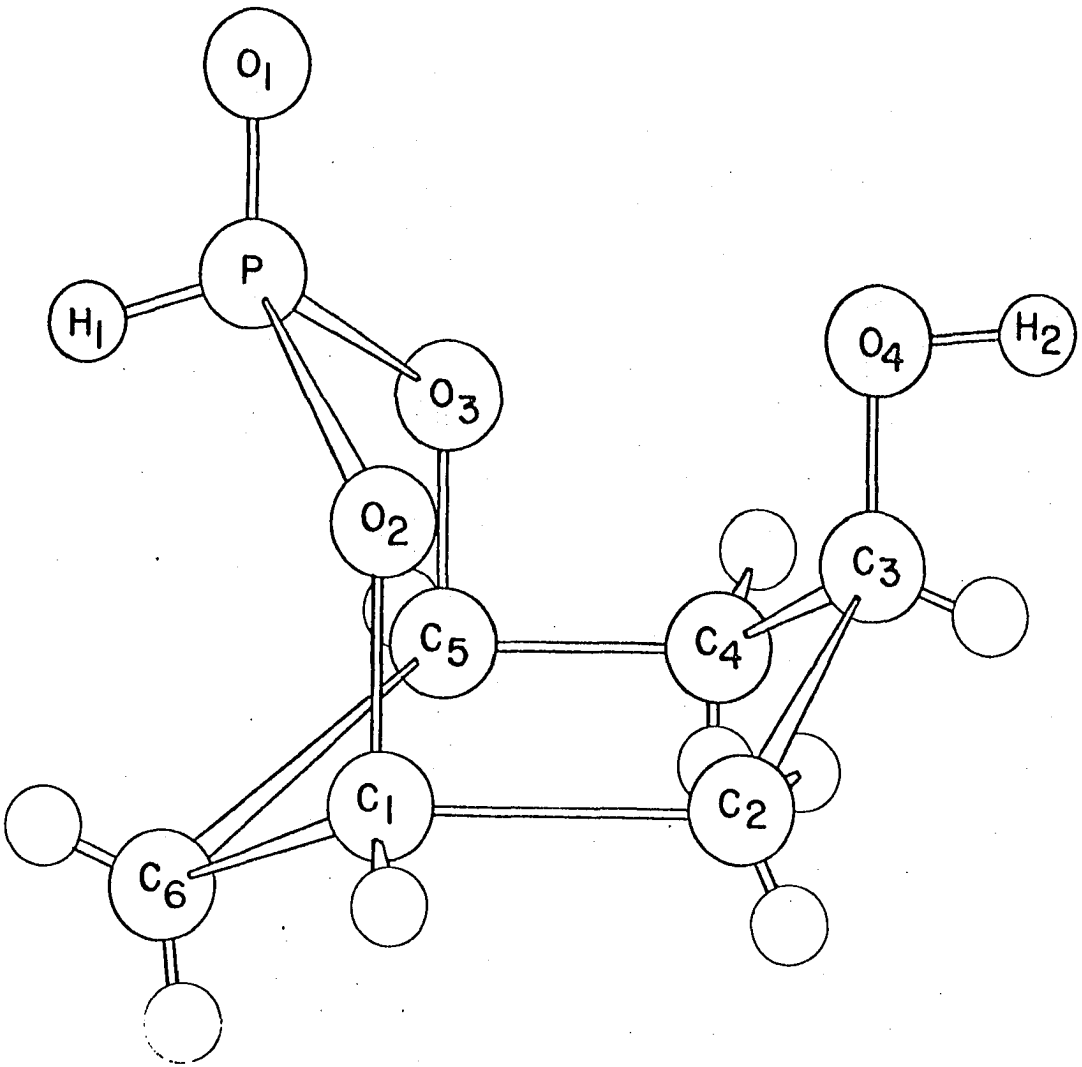

Figure 6. The molecular configuration and conformation of isomer A

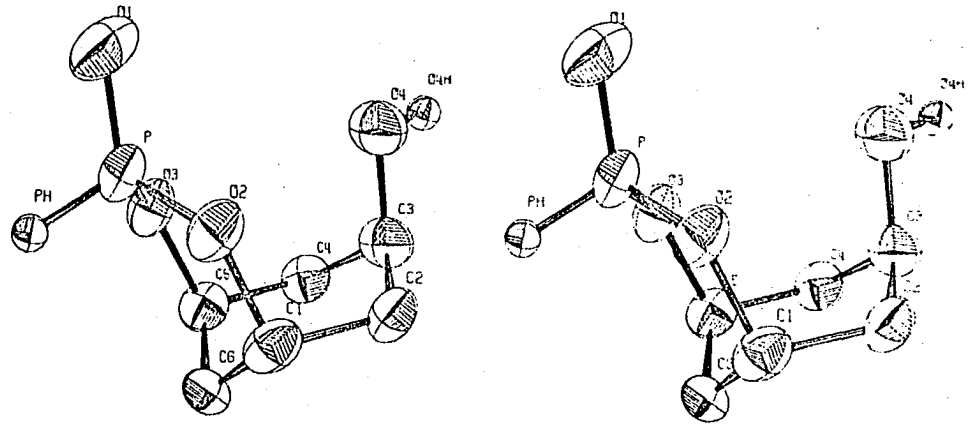

Figure 7. Stereoscopic view of the molecular structure and 50 °/o probability thermal ellipsoids of isomer A

Table 5. Interatomic distances and angles and their standard errors

Bond Distances			Bond Angles		
Atoms	Distance	Standard Error	Atoms	Angle	Standard Error
O_1-P	1.420	0.006	O_1PO_2	114.4	0.3
O_1-P[a]	1.446	0.006	O_1PO_3	114.6	0.3
P-O_2	1.550	0.005	O_2PO_3	107.5	0.2
P-O_3	1.549	0.005	PO_2C_1	121.8	0.4
O_2-C_1	1.468	0.008	PO_3C_5	121.6	0.4
O_3-C_5	1.476	0.008	$O_2C_1C_2$	108.1	0.5
O_4-C_3	1.403	0.009	$O_3C_5C_4$	108.9	0.5
C_1-C_2	1.507	0.009	$O_2C_1C_6$	109.8	0.5
C_2-C_3	1.541	0.009	$O_3C_5C_6$	109.2	0.6
C_3-C_4	1.501	0.010	$O_4C_3C_2$	108.5	0.6
C_4-C_5	1.512	0.009	$O_4C_3C_4$	113.4	0.6
C_5-C_6	1.503	0.009	$C_1C_2C_3$	114.2	0.5
C_6-C_1	1.495	0.010	$C_2C_3C_4$	113.0	0.6
O_4-O_1'[b]	2.816	0.007	$C_3C_4C_5$	115.6	0.6
			$C_4C_5C_6$	111.2	0.6
			$C_5C_6C_1$	110.1	0.6
			$C_6C_1C_2$	112.6	0.6

[a]Interatomic distances averaged over thermal motion. O_1 is assumed to ride on P (56). The effects of thermal motion on all other interatomic distances was never more than 0.007A.

[b]O_1' is related to O_1 by the screw axis in y.

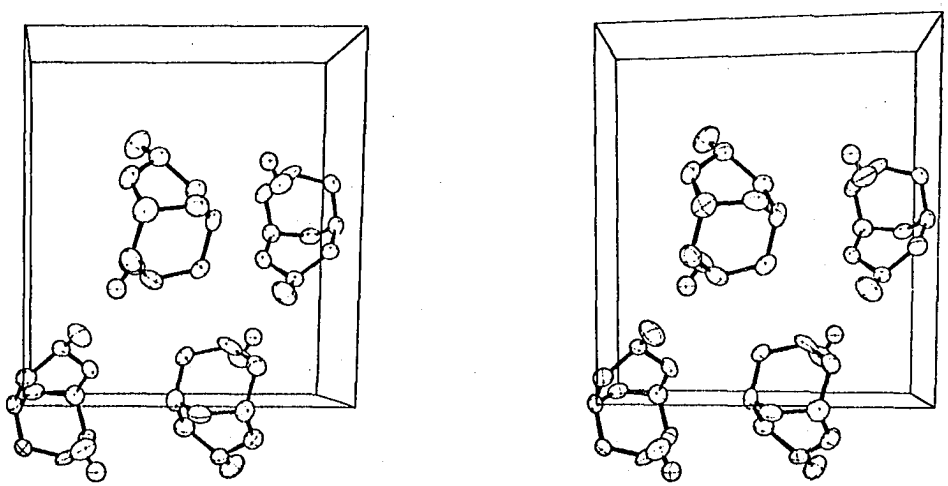

Figure 8. Stereoscopic drawing of the packing of isomer A. The c axis is horizontal and the b axis is vertical

and not between O_4 and O_2 and O_5.

It may be seen qualitatively in the thermal-ellipsoid plots and quantitatively in the anisotropic temperature parameters (Table 4) and the calculated root mean square displacements that of all the atoms, O_1 has the largest thermal motion. The effect of thermal motion on the estimation of bond lengths from x-ray diffraction measurements has been discussed by Busing and Levy (56). They argue from the point of view that the most meaningful interatomic distance is the mean separation of the atoms. They have derived two expressions for thermal motion correction. One expression assumes that one atom of a bonded pair "rides" on the other and is applicable when the riding atom is much lighter than the other and is, in addition, strongly bonded to the other atom. The second expression assumes the atoms move independently. The first case seems most appropriate for the $P{=}O_1$ system. However, both corrections were computed and each gave the same correction (0.026 A). Corrections for all of the other bond distances, assuming the atoms move independently, were computed, but no correction was greater than 0.007 A.

The final value of the z coordinate of C_3 appears to be anomalous. The shift from its final value of several standard deviations in negative z direction tends to not only equalize the C_3-C_2 and the C_3-C_4 distances to the

average C-C distance in the structure but also to equalize the O_4-C_3-C_2 and O_4-C_3-C_4 angles. Various attempts were made to isolate a portion of the data responsible for its position or to find a chemically reasonable explanation of final position, but they were unsuccessful. For example, structure factor calculations were made on the refined parameters and also on the refined parameters except for the z coordinate of C_3 which was shifted negatively to a "more reasonable" value. The number of reflections for which δ

$$\delta = \frac{Fo-Fc}{\sigma}$$

improved by an amount greater than an arbitrary value, ϵ, with the shift in z were counted and were compared with the number which became worse by ϵ or more for the same shift. Furthermore, the magnitudes of Fo and Fc were compared. The results were that the δ's improved by ϵ or more for 102 reflections of which 60 had Fc>Fo and 42 had Fo>Fc, and that the δ's got worse by ϵ or more for 118 reflections of which 65 had Fo>Fc and 53 had Fc>Fo.

Discussion

The structure fully confirms the postulated conformation and configuration of isomer A. Furthermore, it strongly suggests that the proposed structure of isomer B is also correct. Of the two six membered rings in the structure the

phosphorus-containing one is in the boat form. It was was originally thought that for isomer B this boat form could be stabilized by hydrogen bonding between the phosphoryl oxygen and the equitorial hydrogen of the methylene group below the phosphorus. Calculations based on the structure of isomer A seem to indicate otherwise. Assuming that the O=P-O angle and that the P=O distance in isomer B are the same as that found in isomer A (114.5° and 1.44 A, respectively), the O···C distance is 3.44 A. Additional calculations showed that decreasing the O=P-O angle to 110° shortened the O···C distance by only 0.2 A. Although the energy requirements for such flexing are not known, it is doubtful that there could be enough energy gained by hydrogen bonding to pay for it, especially since an alkane-type CH group is a very poor participant in hydrogen bonding.

The boat form of the phosphorus containing ring is probably due first of all to the steric hinderances between the phosphoryl group and the alcoholic group which would prohibit a chair configuration for both the cyclohexane ring and the phosphorus-containing ring. It is probably more energetically favorable for the phosphorus ring to do the flipping than for the cyclohexane ring because hybridizational changes necessary at the intermediate stages are more easily made on the hinging oxygens than they are on four-

covalent carbon atoms. A comparison of the angles and amount of flipping might be analgous to the phosphite $P(OCH_2)_3CCH_3$ and its reaction product with Br_2 (57) in

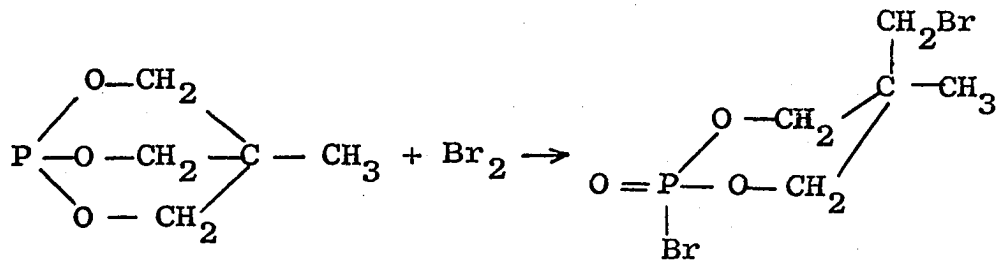

which the flexing occurs at the oxygens. In comparing the parameters of the product with those of the phos-oxide structure it can be seen that less of an arc is involved in flipping the OPO plane. In addition, in the flipping of the carbon ring in isomer A unfavorable steric interactions occur in the eclipsing of several hydrogens. In cyclohexane, for example, the energy barrier for flipping from the chair form to the boat form is about 10 kilocalories of which only about 4.5 kcal are recovered in the boat form (58). Flipping of the OPO plane should involve almost no steric hinderance of the type involved at the carbons.

The structural parameters of the parent caged phosphite of isomer A have been measured by x-ray diffraction in the structure determination of the coordination compound $[Ni(P(OCH)_3(CH_2)_3)_5](ClO_4)_2$ (59, 60, 61). One would assume that the changes in the parameters in going from the coordinated species to the free phosphite would be small, and that the parameters might, therefore, be used accordingly.

The OPO angle (107.5°) and the average POC angle (121.7°) found in isomer A are larger than those found by Riedel (103.5 and 116°, respectively). If his values are representative of the free phosphite it appears that in its hydrolysis to isomer A some strain in these angles is relieved; POC angles for uncyclized methoxy groups in phosphates, for example, have been recently reported with values near 120° (32, 33).

The multiple bond character of the P-O ring system as evidenced by the shortening of the P-O bond distance from the single bond value of the sum of the covalent radii has been discussed in the phos-oxide structure. It is interesting to note that isomer A has POC angles closer to 120° than does phos-oxide and correspondingly shorter P-O distances which supports the proposed bonding description discussed earlier.

The values of the phosphorus-oxygen distances and angles found for isomer A are compared with several other P-O systems in Table 6.

Clearly, the hydrolysis of the parent phosphite must occur by some mechanism other than that of its reaction with alkyl halides. The previously mentioned work concerning the Michaelis-Arbuzov reaction with alkyl halides (48, 49) gave well grounded evidence of the structure of the single isomer produced by the reaction. The conclusions of dipole moment and spectral experiments were that the halide occupied an

Table 6. Comparison of phosphorus-oxygen distances and angles of $OP(OCH_2)_3CCH_3$ with various organo-phosphorus compounds

Compound	$OP(OCH_2)_3CCH_3$	Isomer A	$OP(OCH_2)_2(OCH_3)$	$OP(OC(CH_3)_2)_2(OCH_3)$	P_4O_{10}
Reference			33	32	
P=O (A)	1.46 ± .02	1.44 ± .01	1.44 ± .01	1.44 ± .01	1.40 ± .02
P-O (A)	1.57 ± .02	1.55 ± .01	1.57 ± .01	1.58 ± .01	1.61 ± .02
O=P-O (°)	115.0 ± .8	114.5 ± .3	116.7 ± .6[a]	116.7 ± .6[a]	116.5 ± 1.0
			108.7 ± .6[b]	112.6 ± .6[b]	
O-P-O (°)	103.7 ± .6	107.5 ± .2	99.1 ± .6[c]	98.4 ± .5[c]	101.5 ± 1.0
			107.5 ± .6[d]	105.6 ± .7[d]	
P-O-C (°)	115.2 ± 1.1	121.7 ± .4	112.0 ± .9[e]	112.2 ± .8[e]	124.0 ± 1.0[g]
			118.8 ± .9[f]	123.4 ± .9[f]	

[a] To the ring oxygens.

[b] To the methoxy oxygen.

[c] Within the ring system.

[d] Between the ring oxygens and the methoxy oxygen.

[e] For the free methoxy system.

[f] For the free methoxy system.

[g] P-O-P angle.

Table 6. continued

Compound	$OP(OCH_2Ph)_2(OH)$	BBMOD[h]	$Ag(P(OCH_2)_3CCH_3)_4ClO_4$	$Ni(PO_3C_6H_9)_5(ClO_4)_2$ [j]
Reference	34	57	35	61
P=O (A)	1.47 ± .005	1.46 ± .02	--	--
P-O (A)	1.55 ± .004	1.56 ± .01	1.56 ± .01	1.57 ± .03
O=P-O (°)	110.6 ± .2	113.8 ± .9	117.9 ± .6[i]	115.0 ± 1.0[i]
O-P-O (°)	103.8 ± .2	105.5 ± .7	99.9 ± .9	103.5 ± 1.5
P-O-C (°)	120.6 ± .3	119.0 ± 1.0	122.0 ± 1.3	116.0 ± 1.5

[h] 2-Bromo-5-bromomethyl-5-methyl-2-oxo-1,3,2-dioxaphosphorinane.

[i] M-P-O angle.

[j] $[Ni(P(OCH)_3(CH_2)_3)_5](ClO_4)_2$

equatorial position on the ring in contrast with the axial alcoholic group in isomer A. In the Michaelis-Arbuzov reaction with RX an initial partial bond is made between

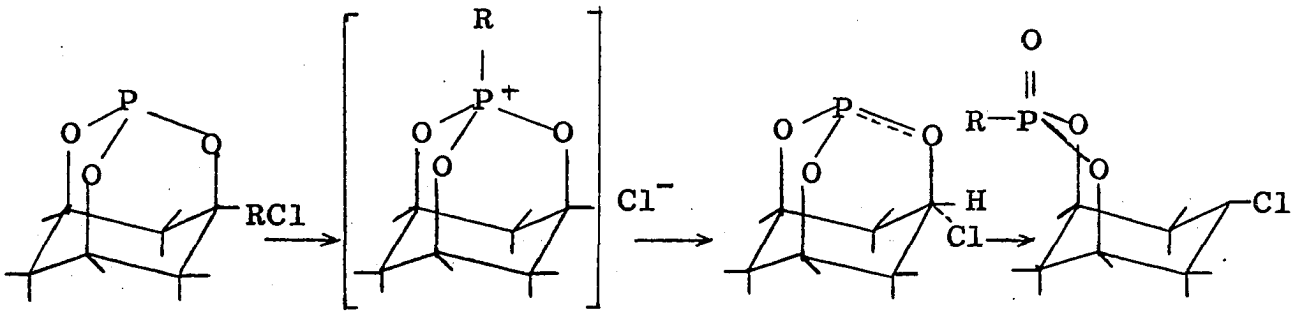

the phosphorus and the alkyl carbon forming in a quasi-phosphonium salt is expected as shown (62, 63). A Sn_2 attack by the halide on the ring carbon could then cause the C-O bond to sever, and the phosphoryl group could then flip into the boat form.

This type of mechanism has been assumed by Arbuzov (64, 65) in the hydrolysis of trialkyl phosphite. An important feature of the proposed mechanism, as is shown, is that the oxygen of the water is carried away as the alcohol:

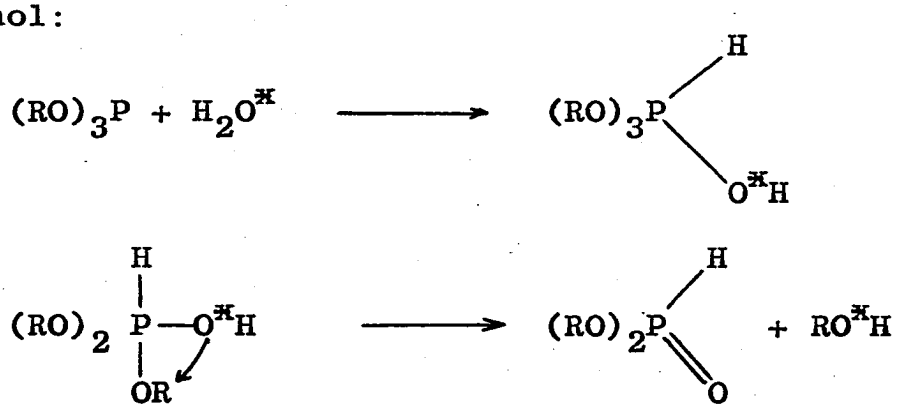

However, kinetic studies and isotopic labeling led Aksnes and Aksnes (66) to reject such a mechanism for the hydrolysis of tripropyl phosphite. Their experiments with ^{18}O-enriched water revealed that the labeled oxygen, as evidenced by displacements of the infrared P=O stretching bands, ended up as the phosphoryl oxygen. They suggested a plausible mechanism which was consistent with their kinetic data which indicated the reaction obeyed an overall third order rate equation, first order in the phosphite and second order in the water. Such a mechanism seems applicable for the hydrolysis of the bicyclic phosphite to isomers A and B. In contrast to the Arbuzov RX cage opening which can produce but a single isomer from this phosphite, the Aksnes type mechanism, shown in Figure 9, can allow for rearrangements at the phosphorus during an intermediate stage to account for the isomerism.

The same type kinetic studies and isotopic labeling experiments as carried out by Aksnes and Aksnes would be in order and, in fact, are in progress* to test the proposed mechanism of this hydrolysis reaction.

---

*J. G. Verkade, Ames, Iowa, Department of Chemistry, Iowa State University of Science and Technology. Current research. Private Communication. 1967.

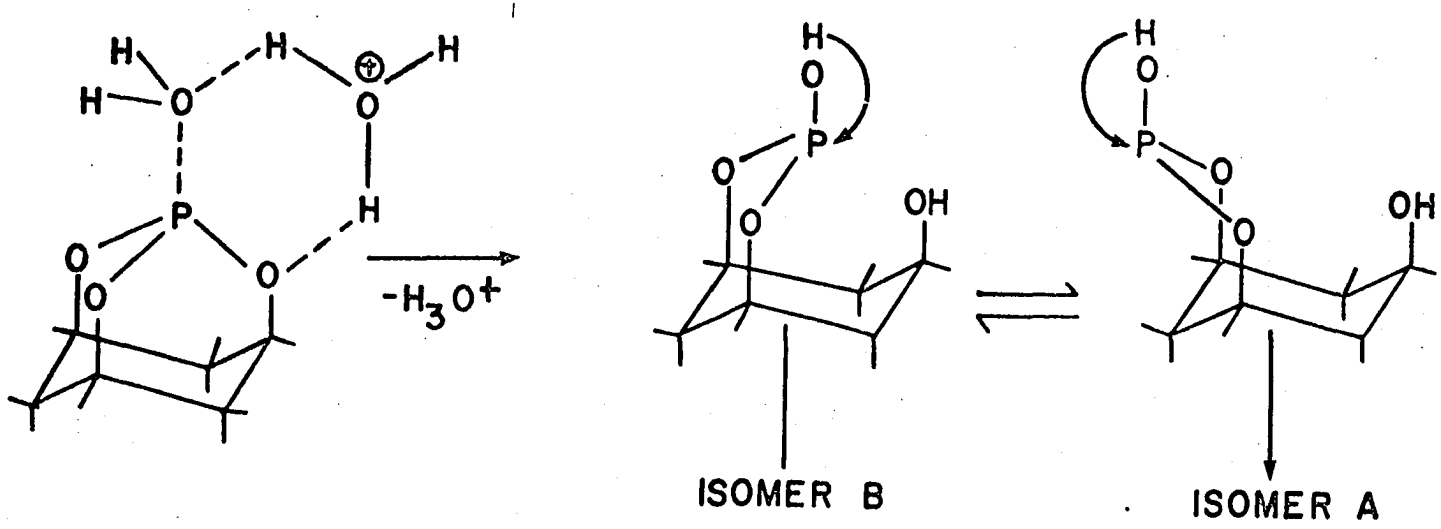

Figure 9. The proposed mechanism for the acid-catalyzed hydrolysis of 2,8,9-trioxa-1-phospha-adamantane

SUGGESTIONS FOR FUTURE WORK

A determination of the structure of one of the Arbuzov products of the reaction of 2,8,9-trioxa-1-phospha-adamantane with RX would provide information concerning the stereochemistry of this important class of reactions. With the careful IR and n.m.r. work that has been done on this type of compound in conjunction with the structures discussed in this report, it is pretty certain that the predicted conformation and configuration would be confirmed. Nevertheless, since a variety of RX may be used, the problem could be chosen to be a simple and straightforward heavy-atom problem with a suitable choice of X(CH_3I, for example, forms a crystalline product with the adamantane-like caged phosphate). Likewise, a lighter X could be chosen in order to obtain more accurate distances and angles not involving X.

It might be of interest to pursue the electrical properties of the phos-oxide compound more extensively. The pursuit would probably involve only a more thorough literature study of crystalline electrets than has been carried out by this author. It would seem, however, that such a large value of constant polarization as found in phos-oxide would be manifested in some interesting physical properties.

The handling of crystal decomposition in the x-ray beam for both phos-oxide and for isomer A was frustrating in that the particular reflections chosen to monitor the decomposition were apparently not representative of the radiation damage. It would seem logical that it might always be the case that any change in the internal structure would affect each reflection independently. No general guidelines could be found in the literature for handling the problem. It is conceivable that a study of decomposition in some particular cases might aid in proposing some guidelines that would not be altogether compound specific. Perhaps a more watchful eye on the backgrounds would provide an indication of decomposition. Perhaps the only conclusion one could make would be to suggest that film data be used to determine the order in which the counter data be taken.

LITERATURE CITED

1. J. G. Verkade and L. T. Reynolds, J. Org. Chem., 25, 663 (1963).

2. H. Stetter and K. Steinacker, Chem. Ber., 85, 451 (1952).

3. T. J. Huttemann, B. M. Foxman, C. R. Sperati, and J. G. Verkade, Inorg. Chem., 4, 950 (1965).

4. J. G. Verkade, R. E. McCarley, D. G. Hendricker, and R. W. King, Inorg. Chem., 4, 228 (1965).

5. D. G. Hendricker. Metal carbonyl complexes of polycyclic phosphite esters. Unpublished Ph.D. thesis. Ames, Iowa, Library, Iowa State University of Science and Technology. 1965.

6. J. G. Verkade, R. W. King, and C. W. Heitsch, Inorg. Chem., 3, 884 (1964).

7. J. G. Verkade and R. W. King, Inorg. Chem., 1, 948 (1962).

8. J. G. Verkade, T. J. Huttemann, M. K. Fung, and R. W. King, Inorg. Chem., 4, 83 (1965).

9. R. D. Bertrand, G. K. McEwen, E. J. Boros, and J. G. Verkade, [Stereochemistry in the reaction of bicyclic phosphite esters with organic halides and halogens, to be published in J. Am. Chem. Soc., 90 (1968)].

10. S. G. Goodman and J. G. Verkade, Inorg. Chem., 5, 498 (1966).

11. N. F. M. Henry and K. Lonsdale, eds. International tables for x-ray crystallography. Vol. 1. Birmingham, England, Kynoch Press. 1952.

12. D. E. Williams, U.S. Atomic Energy Commission Report IS-1052, [Iowa State University of Science and Technology, Ames. Institute for Atomic Research] (1964).

13. M. E. Maurice, Proc. of the Cambridge Phil. Soc., 26, 491 (1930).

14. P. J. Wheatley, J. Chem. Soc., 2206 (1964).

15. T. C. Furnas. Single crystal orienter instruction manual. Milwaukee, Wisconsin, General Electric Co. 1957.

16. D. E. Williams and R. E. Rundle, J. Am. Chem. Soc., 86, 1660 (1964).

17. M. Ledet, U.S. Atomic Energy Commission Report IS-876, [Iowa State University of Science and Technology, Ames. Institute for Atomic Research] (1964).

18. H. P. Hanson, F. Herman, J. D. Lea, and S. Skillman, Acta Cryst., 17, 1040 (1964).

19. D. W. J. Cruickshank and D. E. Pilling. Crystallographic calculations on the Ferranti Pegasus and Mark I computers. In R. Pepinsky, J. M. Robertson, and J. C. Speakman, eds. Computing methods and the phase problem in x-ray crystal analysis. pp. 32-78. New York, New York, Pergamon Press. 1961.

20. W. R. Busing, K. O. Martin, and H. A. Levy, U.S. Atomic Energy Commission Report ORNL-TM-306, [Oak Ridge National Laboratory, Oak Ridge, Tennessee] (1964).

21-22. C. K. Johnson, U.S. Atomic Energy Commission Report ORNL-3794, [Oak Ridge National Laboratory, Oak Ridge, Tennessee] (1965).

23. O. Neunhoeffer and W. Maiwald, Chem. Ber., 95, 108 (1962).

24. T. L. Brown, J. G. Verkade, and T. S. Piper, J. Phys. Chem., 65, 2051. (1961).

25. G. S. Zhdanov. Crystal physics. A. F. Brown, ed. and translator. New York, New York, Academic Press. 1965.

26. J. R. Parks, J. Am. Chem. Soc., 79, 757 (1957).

27. C. A. Coulson. Valence. New York, New York, Oxford Press. 1952.

28. N. Muller, P. C. Lauterbur and J. Goldenson, J. Am. Chem. Soc., 78, 3557 (1956).

29. P. A. Akishin, N. G. Rambidi and E. Z. Aasorin, Krystallographiya, 4, 360 (1959).

30. L. R. Maxwell, S. B. Hendricks, and L. S. Deming, J. Chem. Phys., 5, 626 (1937).

31. G. C. Hampson and A. J. Stosick, J. Am. Chem. Soc., 60, 1814 (1938).

32. M. B. Newton, J. R. Cox and J. A. Bertrand, J. Am. Chem. Soc., 88, 1503 (1966).

33. T. A. Steitz and W. N. Lipscomb, J. Am. Chem. Soc., 87, 2488 (1965).

34. J. D. Dunitz and J. S. Rollett, Acta Cryst., 9, 327 (1956).

35. J. V. Ugro. The crystal structure determinations of $Cu_5Cl_{10}(C_3H_7OH)$, $DyCl_3 \cdot 6H_2O$ and $Ag(P(OCH_2)_3CCH_3)_4ClO_4$. Unpublished Ph.D. thesis. Ames, Iowa, Library, Iowa State University of Science and Technology. 1967.

36. L. L. Burger, U.S. Atomic Energy Commission Report HW-44888, [Hanford Atomic Products Operation, Richland, Washington] (1957).

37. M. Margoshes, F. Fillwalk, V. A. Fassel, and R. E. Rundle, J. Chem. Phys., 22, 381 (1954).

38. F. A. Cotton and G. Wilkinson. Advanced inorganic chemistry. New York, New York, Interscience Publishers. 1962.

39. J. M. Jenkins, T. J. Huttemann, and J. G. Verkade, Adv. in Chemistry Series, 62, 604 (1967).

40. J. L. Burdett and L. L. Burger, Can. J. Chem., 44, 111 (1966).

41. F. K. Butcher, B. E. Deuters, W. Gerrard, E. F. Mooney, R. A. Rothenbury, and H. A. Willis, Spectrochimica Acta, 20, 759 (1964).

42. D. L. Venezky and R. B. Fox, J. Am. Chem. Soc., 75, 3967 (1953).

43. D. L. Venezky and R. B. Fox, J. Am. Chem. Soc., 78, 1664 (1956).

44. A. D. Troitskaya, Trudy Kazan., Khim. Tekhnol. Inst. S. M. Kirova, 23, 228 (1957). Original not available. Abstracted in Chem. Abstr. 52, 9951b (1958).

45. L. W. Daasch, J. Am. Chem. Soc., 80 5301 (1958).

46. E. J. Boros, K. J. Coskran, R. W. King, and J. G. Verkade, J. Am. Chem. Soc., 88, 1140 (1966).

47. L. J. Bellamy. The infrared spectra of complex molecules. 2nd. ed. London, Methuen and Co. 1958.

48. K. D. Berlin, C. Hildebrand, J. G. Verkade, and O. C. Dermer, Chem. and Ind., 291 (1963).

49. K. D. Berlin, C. Hildebrand, A. South, D. M. Hellwege, M. Peterson, E. A. Pier, and J. G. Verkade, Tetrahedron, 20 323 (1964).

50. T. J. Huttemann, The chemistry and transition metal complexes of 2,8,9-trioxa-1-phospha-adamantane. Unpublished Ph.D. thesis. Ames, Iowa, Library, Iowa State University of Science and Technology. 1965.

51. J. B. Nelson and D. P. Riley, Proc. Phys. Soc., 57, 160 (1945).

52-53. S. Westman and A. Magnéli, Acta Chem. Scand., 11, 1587 (1957).

54. W. R. Busing, K. O. Martin, and H. A. Levy, U.S. Atomic Energy Commission Report ORNL-TM-305, [Oak Ridge National Laboratory, Oak Ridge, Tennessee] (1962).

55. G. C. Pimentel and A. L. McClellan. The hydrogen bond. San Francisco, California, W. H. Freeman, 1960.

56. W. R. Busing and H. A. Levy, Acta Cryst., 17, 142 (1964).

57. T. A. Beineke, Chem. Comm., 860 (1966).

58. E. L. Eliel. Stereochemistry of carbon compounds. New York, New York, McGraw-Hill. 1962.

59. E. F. Riedel, J. G. Verkade and R. A. Jacobson, [The trigonal bipyramidal structure of a pentakis (alkyl phosphite) nickel(II) perchlorate, to be published in Inorg. Chem., 7 (1968)].

60. E. F. Riedel and R. A. Jacobson, [The crystal structure of $Ni(PO_3C_6H_9)_5(ClO_4)_2$, to be submitted to Inorg. Chem., 7 (1968)].

61. E. F. Riedel. The crystal structure of $Ni(PO_3C_6H_9)_5(ClO_4)_2$. Unpublished M.S. thesis. Ames, Iowa, Library, Iowa State University of Science and Technology. 1966.

62. W. S. Wadsworth and W. D. Emmons, J. Am. Chem. Soc., 84, 610 (1962).

63. A. W. Frank, Chem. Rev., 61, 389 (1961).

64. A. E. Arbuzov, J. Russ. Phys. Chem. Soc., 38, 291 (1906).

65. A. E. Arbuzov and M. G. Imajev, Dokl. Akad. Nauk SSSR, 112, 856 (1956).

66. G. Aksnes and D. Aksnes, Acta Chem. Scand., 18, 1623 (1964).

67. B. L. Laube, R. D. Bertrand, G. A. Casedy, R. D. Compton, and J. G. Verkade, Inorg. Chem., 6, 173 (1967).

68. L. G. Hoard and R. A. Jacobson, J. Chem. Soc. (A), 1203 (1966).

69. L. F. Dahl and R. E. Rundle, J. Chem. Phys., 26, 1751 (1957).

70. D. Harker and J. S. Kasper, Acta Cryst., 1, 70 (1948).

71. D. Sayre, Acta Cryst., 5, 60 (1952).

72. W. Cochran and M. M. Woolfson, Acta Cryst., 8, 1 (1955).

73. F. R. Ahmed. NRC crystallographic program for the IBM/360 system. Ottawa, Canada, Department of Pure Physics, National Research Council. 1966.

74. W. R. Busing and H. A. Levy, Acta. Cryst., 22, 457 (1967).

ACKNOWLEDGMENTS

The author is grateful to Dr. D. R. Fitzwater for his interest and guidance in this research and in the areas of computer usage and x-ray diffraction instrumentation. The author would also like to express his appreciation to Dr. J. G. Verkade for suggesting the research problems and for continuing his interest and support throughout the investigations.

The assistance of Mr. Fred Hollenbeck in the x-ray laboratory is gratefully acknowledged. For the many helpful discussions concerning the theory and practice of x-ray diffraction the members of the x-ray chemistry groups over the past years are thanked.

Finally, the author would like to thank his wife, Sunni, for her continued support during graduate school and for her help in the preparation of this manuscript.

APPENDIX A. THE SPACE GROUP DETERMINATION AND ITS IMPLICATIONS OF $OP(N(CH_3)CH_2)_3CCH_3$

Introduction

A structural analog of the phos-oxide compound which has aroused some chemical interest is 1-oxo-2,6,7-trimethyl-4-methyl-2,6,7-triaza-1-phosphabicyclo[2.2.2]octane. The proposed structural relationship to phos-oxide, made obvious in the following diagram, is that the bridging oxygens of the phos-oxide are replaced by $N-CH_3$ groups.

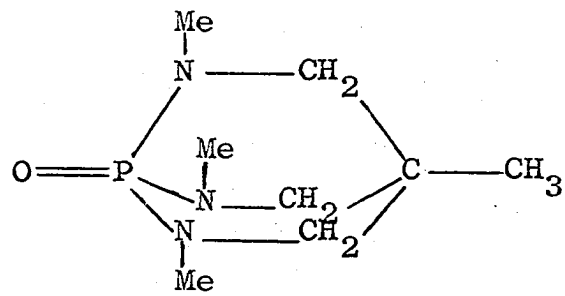

The molecule is apparently the same bicyclic, football shaped molecule with the probable retention of the threefold axis running through the molecule.

The chemical interest arises from the bidentate ligand properties of its parent phosphite and from the results of n.m.r. spectra, which together with the preparation of the compound, have been reported by Laube, et al. (67). They found the NCH_3 groups to be equivalent with respect to coupling of the P^{31} nucleus with their protons. The implication is that either the NR_3 configuration is locked

in a puckered arrangement, or the CH_3 group is rapidly interchanging with the lone pair of electrons on the N, or the NR_3 group is planar with a sp^2 type bonding orbital arrangement on the N.

Low temperature n.m.r. data indicated that there was no disorder locked into the molecule at lower temperatures which might be taken as evidence for the lack of inversion. On the other hand, the existence of planar NR_3 groups in cyclophosphonitriles is known. Recently, for example, Hoard and Jacobson reported the crystal structure of N-Methyltrichlorophosphinimine dimer (68) diagramatically displayed as follows:

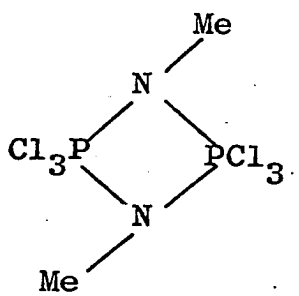

The two P's, the N and the methyl carbon are all in the same plane.

It was felt that if crystallographic evidence could be found supporting the planar configuration it would be a worthwhile contribution to the chemical literature concerning this class of compounds.

Structural Implications of Space Groups

It was noted that if the NR_3 part of this molecule was indeed planar there would exist a mirror plane coincident with the threefold rotational axis of the molecule. It would therefore be possible, although by no means necessary, for nature to make use of this mirror in the crystallization process for this compound. The close example of this is, of course, the phos-oxide molecule which crystallizes such that its molecular mirror is coincident with the mirror plane of the crystallographic space group.

Incorporation of molecular symmetry into the space group symmetry is a common occurrence. Furthermore, the detection of this phenomena can usually be accomplished experimentally by merely determining the space group, unit cell size, and number of molecules per unit cell. Taking these facts into account with the expected molecular symmetry—and the general size and shape of the molecule, one can make an attempt to conclude into which set of space group positions the molecule resides. For example, suppose that this particular compound crystallizes in a space group which contains a mirror and N general positions. Furthermore, suppose that the number of molecules per unit cell is N/2. One could then conclude that the molecule lies on the crystallographic mirror, must therefore contain a molecular mirror, and must therefore have a planar NR_3 group, since

there is no other apparent molecular symmetry other than the threefold axis.

Such an approach, it should be pointed out, is not without some pitfalls. First of all, the approach assumes that the general structure of the molecule is known whereas in fact that is what is to be determined. Secondly, this approach assumes that there is no disorder in the crystallization process. This has been seen, historically, to be a dangerous assumption. The longly disputed trimeric iron tetracarbonyl structure was thought to be linear with respect to the three irons because space group considerations implied a center of symmetry within the molecule. Dahl and Rundle (69) discussed this and gave crystallographic evidence of disorder in the form of shifted triangles of irons in a regular hexagon (with a center of symmetry). Later work has confirmed the triangular arrangement.

In terms of numbers, however, conclusions from this approach have usually turned out to be correct. In view of the chemical interest in the compound the elucidation of the space group was undertaken with this approach in mind. It was felt that even if no structural conclusions could be made from the space group the work might not be wasted in that the undertaking of a full crystallographic structure determination is being considered anyway. A determination of the space group at this point would shed light on the expected degree of difficulty of the crystal structure determination

and would thereby have a bearing on a decision as to whether or not to support the full scale determination.

Experimental

Since the compound was reportedly hygroscopic, single crystals, provided by Mr. B. L. Laube from the synthesis mentioned earlier (67), were mounted in sealed Lindemann glass capillaries. The mounting was done in a dry nitrogen atmosphere inside a vacuum drybox. It should be mentioned, however, that later when one of the capillaries was accidentally broken, exposing the crystal to the atmosphere, only very slow decomposition with time was revealed in the subsequent x-ray photographs. This indicates that reasonable success would be expected if one mounted the crystals under room conditions and then evacuated and sealed the capillary when he was through.

The crystal was aligned on a Weissenberg camera, and zero through fourth layer Weissenberg photographs were taken. The diffraction symmetry was observed to be m m m (orthorhombic). The conditions for non-extinction were as follows:

h k ℓ	none
h k 0	h = 2n
h 0 ℓ	ℓ = 2n
0 k ℓ	k = 2n.

Accordingly, the assignment of the space group Pbca, which uniquely satisfies these conditions, was made.

Lattice constants, calculated from Weissenberg and rotation photographs, were as follows:

$$a = 13.15 \text{ A}$$

$$b = 13.49 \text{ A}$$

$$c = 12.99 \text{ A}$$

$$\text{volume} = 2306 \text{ A}^3$$

The lattice constant data was not calibrated and the results have an estimated uncertainty of 0.07 A.

The density of the crystals was bracketed between 1.0 and 1.4 gms/cm^3 on the basis of observing the floatation properties in 1-bromo-propane and in H_2O. Such a density is consistant with the expectation that the density should be similar but slightly less than the phos-oxide compound (1.53 gms/cm^3). The calculated density for eight molecules per unit cell is 1.17 gms/cm^3.

Conclusions

Space group Pbca has eight general positions and two sets of special positions. The special positions are centers of symmetry. Since there is no molecular center of symmetry, one is forced to conclude that the molecules lie in general positions. Hence, it is impossible to make a conclusion concerning the planarity of the NR_3 group from space group considerations.

Remarks Concerning Full Scale Structure Determination

Excluding hydrogens there are 13 atomic positions to be determined. Certainly, as a crystal structure determination

problem, it could not be classified as complex. Furthermore, if the structure is solved, the three NR_3 group measurements are crystallographically independent and should yield more reliable conclusions with respect to the planarity as well as three independent, but chemically equivalent, P-N distances and related angles.

As with the phos-oxide compound, many of the interatomic vectors are parallel, and it may be difficult to solve the phase problem with conventional Patterson techniques of either analyzing the Harker lines or performing a general superposition. Because of the expected overlap it may be impossible to distinguish a P-P vector on a Harker line even though the problem borders on a heavy atom problem. (The general rule of thumb for such an approach is

$$\frac{(\text{atomic number of P})^2}{\Sigma(\text{at. no. of the rest})^2}$$

be greater than 0.5--the ratio is 0.44 for this compound.)

If one would be successful in determining a P position it is quite doubtful that it alone would dominate the signs of the structure factors enough to permit one to go directly to Fourier techniques. However, one superposition of the Patterson map using a minimum function should successfully solve the Patterson if the superposition point (u, v, w) is chosen as follows: $u = 2x$, $v = 2y$, $w = 2z$, where x, y and z are the fractional coordinates of the P in electron

density space.

If the phosphorus could not be located from the Patterson map, it is this author's suggestion that statistical direct methods for determining the signs of the structure factors be employed for solving the phase problem. This approach is suggested first of all because of the expected overlap and subsequent ambiguities of the Patterson map. Secondly, the fact that the compound crystallizes into a unique centrosymmetric space group with all atoms in general positions removes some of the problems of the direct method approach and gives a fairly high probability of success for the approach.

The total number of atoms per unit cell, and not the number per asymmetric unit, limits the degree of complexity of structure determinations by direct methods. It would be expected that for a crystal of this complexity with eight 13-atom molecules in the unit cell too many of the structure factors would be small, rendering the use of strict Harker-Kasper inequalities (70) ineffective in determining the structure. However, the basic sign relationship of Sayre (71), $s(\vec{h})s(\vec{h}')s(\vec{h}+\vec{h}') = +1$, where $\vec{h}$ and $\vec{h}'$ are the Miller indices of any two reflections, which is true for large structure factors and can be derived from Harker-Kasper inequalities, is "probably" true for smaller structure factors. A quantitative expression for this probability has

been sought by several workers. Cochran and Woolfson (72) have derived the following expression for the probability of Sayre's equation holding true:

$$P_+ (\vec{h},\vec{h}') = 1/2 + 1/2 \tanh \frac{\epsilon_3}{\epsilon^3} \; |U_{\vec{h}} U_{\vec{h}'} U_{\vec{h}+\vec{h}'}|$$

where U is the unitary structure factor

$$\epsilon = \sum_{j=1}^{N} n_j^2 \quad (n_j \text{ is the unitary scattering factor})$$

$$\epsilon_3 = \sum_{v=1}^{N} n_j^3$$

The use of this expression and others have been programmed for the computer. The National Research Council of Canada, for example, has a well documented program (73) which is available for general use. It is felt that only a moderate amount of work would be required to set up and hopefully solve this structure with such an approach.

APPENDIX B. AN ALGORITHM FOR THE TUNING OF A GENERAL DIFFRACTION MAXIMA ON AN AUTOMATED FOUR-CIRCLE DIFFRACTOMETER

A diffracted beam of x-rays or neutrons of a particular reflection is said to be tuned when the crystal and detector are positioned such that not only is the diffracted beam of maximum intensity but also that the maximum strike the center of the detecting system. The tuning of a general reflection on a typical single crystal orienter (15, 74) by some iterative process of adjusting the three crystal orienting rotational axes, chi, phi, and omega, and the detector axis, theta, is a process that is surprisingly difficult to define. One can easily get into an iterative process that can be carried on indefinitely without ever converging on the solution.

With a computer intimately available during the tuning process it has been possible to define an algorithm which will converge for any general reflection. Furthermore, the operations required in terms of shaft movements are very simple if one can make some arithmetic calculations during the process.

It was noted that when a crystal is in a position to diffract the "reflecting" plane (to which the diffraction vector is normal) is vertical. It was further noted that

omega axis* is always vertical and is hence parallel with the plane, and that the chi axis is perpendicular to the omega axis and is nearly parallel with the plane if omega is nearly equal to the Bragg angle, theta. The upshot is that any plane can be properly positioned with chi and omega adjustments to give a maximum intensity in the horizontal plane within which the detector swings. This means that a general peak can be tuned by a iterative process of the following three steps:

1. Maximize the total intensity with respect to omega adjustments.
2. Center the diffracted beam with respect to top-bottom beam splitters on the detector face with adjustments in chi.
3. Center the detector on the diffracted beam with respect to left-right beam splitters on the detector face with adjustments in theta.

Phi is left out of the tuning process because it in general is not parallel or perpendicular to the reflecting plane, and only two axes are necessary to orient the reciprocal lattice vector. In particular, phi is parallel to the reflecting plane at chi = 0° and is normal to the

*The axis lables, omega, chi, phi and theta are used in the conventional definition for single orientor units. See references 15 or 74, for example.

reflecting plane at chi = 90° providing omega = theta, but it is in between for the rest of the cases.

The chi-omega tuning process will in general leave omega at some value other than the value of theta. The computer can then be used to calculate the chi and phi adjustments necessary to compensate for a rotation of omega to the Bragg angle. The derivation of the expressions for the compensating amounts will now be presented.

The following reference coordinate system will be used throughout the derivation. Consider a crystal in position to diffract.

$\vec{r}_1$ is coincident with the diffraction vector, normal to the "reflecting" plane, bisecting the incident and diffracted beams.

$\vec{r}_3$ is coincident with the vertical instrument axis omega.

$\vec{r}_2$ is mutually perpendicular to $\vec{r}_1$ and $\vec{r}_3$ and is in the direction to make a right handed set.

Note that if omega = theta $\vec{r}_2$ coincides with the chi axis. Furthermore, at chi = zero $\vec{r}_3$ and the phi axis are coincident. Moreover, the senses of $\vec{r}_2$ and $\vec{r}_3$ are the same as those under which chi and phi physically move.

A reciprocal lattice vector $\vec{x}$ may be brought into coincidence with the diffraction vector $\vec{d}$ of a given reflection (i.e. the crystal is brought into position to diffract) with appropriate phi, chi and omega rotations of

ϕ, χ and $-\Delta\omega$ from phi=0, chi=0 and omega = the Bragg angle.

It is again noted that in the initial conditions the phi and chi axes are coincident with $\vec{r_3}$ and $\vec{r_2}$ respectively and that the chi-$\vec{r_2}$ coincidence is independent of phi rotation. Hence, rotation of phi, chi and omega in that order may be done straightforwardly in the basic coordinate system.

$$\vec{d} = R(-\Delta\omega)R(\chi)R(\phi)\vec{x}$$

where the R's are the rotation operator matrices in the basic coordinate system.

$$R(-\Delta\omega) = \begin{pmatrix} \cos-\Delta\omega & \sin-\Delta\omega & 0 \\ -\sin-\Delta\omega & \cos-\Delta\omega & 0 \\ 0 & 0 & 1 \end{pmatrix} = \begin{pmatrix} \cos\ \Delta\omega & -\sin\ \Delta\omega & 0 \\ \sin\ \Delta\omega & \cos\ \Delta\omega & 0 \\ 0 & 0 & 1 \end{pmatrix}$$

$$R(\chi) = \begin{pmatrix} \cos\ \chi & 0 & \sin\ \chi \\ 0 & 1 & 0 \\ -\sin\ \chi & 0 & \cos\ \chi \end{pmatrix}$$

$$R(\phi) = \begin{pmatrix} \cos\ \phi & \sin\ \phi & 0 \\ -\sin\ \phi & \cos\ \phi & 0 \\ 0 & 0 & 1 \end{pmatrix}$$

It should be noted at this point for later manipulations that for this type of rotation matrices

$$R(-\alpha) = R(\alpha)^{-1} = R(\alpha)^{T}.$$

The omega = theta solution of the problem occurs at $(0, \chi_o, \phi_o)$. Hence, in addition

$$\vec{d} = R(\chi_o)R(\phi_o)\vec{x}.$$

$$\vec{x} = (R(-\Delta\omega)R(\chi)R(\phi))^{-1}\,\vec{d} = (R(\chi_o)R(\phi_o))^{-1}\,\vec{d}$$

$$= R(-\phi)R(-\chi)R(\Delta\omega)\vec{d} = R(-\phi_o)R(-\chi_o)\vec{d}.$$

Since $\vec{d}$ is coincident with $\vec{r}$ and may be regarded as a unit vector it may be represented by $\begin{pmatrix}1\\0\\0\end{pmatrix}$.

$$\therefore \vec{x} = \begin{pmatrix}\cos\phi & -\sin\phi & 0\\ \sin\phi & \cos\phi & 0\\ 0 & 0 & 1\end{pmatrix}\begin{pmatrix}\cos\chi & 0 & -\sin\chi\\ 0 & 1 & 0\\ \sin\chi & 0 & \cos\chi\end{pmatrix}\begin{pmatrix}\cos\Delta\omega & \sin\Delta\omega & 0\\ -\sin\Delta\omega & \cos\Delta\omega & 0\\ 0 & 0 & 1\end{pmatrix}\begin{pmatrix}1\\0\\0\end{pmatrix}$$

$$= \begin{pmatrix}\cos\phi_o & -\sin\phi_o & 0\\ \sin\phi_o & \cos\phi_o & 0\\ 0 & 0 & 1\end{pmatrix}\begin{pmatrix}\cos\chi_o & 0 & -\sin\chi_o\\ 0 & 1 & 0\\ \sin\chi_o & 0 & \cos\chi_o\end{pmatrix}\begin{pmatrix}1\\0\\0\end{pmatrix}$$

yielding

$$x_1 = \cos\phi\cos\chi\cos\Delta\omega + \sin\phi\sin\Delta\omega = \cos\phi_o\cos\chi_o \quad \text{(I)}$$

$$x_2 = \sin\phi\cos\chi\cos\Delta\omega - \cos\phi\sin\Delta\omega = \sin\phi_o\cos\chi_o \quad \text{(II)}$$

$$x_3 = \sin\chi\cos\Delta\omega = \sin\chi_o \quad \text{(III)}$$

These three equations contain the solution for the compensating chi and phi adjustments for a theta-omega difference of $\Delta\omega$. The chi correction is given directly by III:

$$\sin\chi_o = \sin(\chi + \Delta\chi) = \sin\chi\cos\Delta\omega \quad \text{(IV)}$$

where χ is the tuned chi value and χ_o is the corresponding chi value at omega = theta. $\Delta\chi$, therefore, is the chi correction.

Dividing II by I gives an expression for tan ϕ_o:

$$\tan \phi_o = \frac{\sin \phi \cos \chi \cos \Delta\omega - \cos \phi \sin \Delta\omega}{\cos \phi \cos \chi \cos \Delta\omega + \sin \phi \sin \Delta\omega} .$$

Dividing numerator and denominator by cos ϕ cos χ cos $\Delta\omega$ have

$$\tan \phi_o = \frac{\tan \phi - \frac{\tan \Delta\omega}{\cos \chi}}{1 + \frac{\tan \Delta\omega \tan \phi}{\cos \chi}} . \qquad \text{(V)}$$

But also $\tan \phi_o = \tan (\phi + \Delta\phi) = \dfrac{\tan \phi + \tan \Delta\phi}{1 - \tan \Delta\phi \tan \phi}$. (VI)

Equating V and VI have

$$\tan \Delta \phi = - \frac{\tan \Delta\omega}{\cos \chi} . \qquad \text{(VII)}$$

Although VII is a compact, simple expression to evaluate, its derivation required division by cos χ, and is thereby rendered invalid at $\chi = 90°$. An alternative expression was developed without any such invalid intermediate steps and is presented here, also.

I times II gives

$\sin \phi \cos \phi \cos^2\chi \cos \Delta\omega + \sin^2\phi \cos \chi \cos \Delta\omega - \cos^2\phi \cos\chi$
$- \cos^2\phi \cos \chi \cos \Delta\omega \sin \Delta\omega - \sin \phi \cos \phi \sin^2\Delta\omega =$
$\cos \phi_o \sin \phi_o \cos^2\chi_o$.

Replacing sin ϕ cos ϕ with $\frac{\sin 2\phi}{2}$, collecting terms and replacing $\cos^2\phi - \sin^2\phi$ with cos 2ϕ, and finally dividing through by $\cos^2\Delta\omega$ have

$$\sin 2\phi(\cos^2\chi - \tan^2\Delta\omega) - 2\cos \chi \tan \Delta\omega \cos 2\phi = \frac{\sin 2\phi_o \cos \chi_o}{\cos^2\Delta\omega}.$$

But from III

$$\cos^2\chi_o = 1 - \sin^2\chi \cos^2\Delta\omega, \text{ giving}$$

$$\frac{\cos^2\chi_o}{\cos^2\Delta\omega} = \tan^2\Delta\omega + \cos^2\chi.$$

$$\therefore \sin 2\phi_o = \frac{\sin^2\phi\ (\cos^2\chi - \tan^2\Delta\omega) - 2\cos\chi \tan\Delta\omega \cos 2\phi}{\cos^2\chi + \tan^2\Delta\omega}.$$

Letting $k = \frac{\cos\chi}{\tan\Delta\omega}$ have

$$\sin 2\phi_o = \frac{k^2 - 1}{k^2 + 1} \sin 2\phi - \frac{2k}{k^2 + 1} \cos 2\phi. \quad \text{(VIII)}$$

But also

$$\sin 2\phi_o = \sin(2\phi + 2\Delta\phi) = \sin 2\phi \cos 2\Delta\phi + \cos 2\phi \sin 2\Delta\phi. \quad \text{(IX)}$$

Equating the coefficients of sin 2ϕ and of cos 2ϕ gives a valid solution to equations VIII and IX simultaneously for all values of k, yielding

$$\cos 2\Delta\phi = \frac{k^2 - 1}{k^2 + 1} \quad \text{(X)}$$

$$\sin 2\Delta\phi = \frac{-2k}{k^2 + 1} \quad \text{(XI)}$$

It may be seen that the necessary condition $\cos^2 2\Delta\phi + \sin^2 2\Delta\phi = 1$ is upheld.

Of the two solutions satisfying XI at chi = 90°, $\Delta\phi$ = 0° and $\Delta\phi$ = 90°, the latter one is applicable. It may be seen that the $\Delta\phi$ correction ranges from $-\Delta\omega$ at χ = 0° to 90° at χ = 90°. The range of $\Delta\chi$ is 0° at χ = 0° to $\Delta\omega$ at χ = 90°. The expressions IV and XI are valid for $\pm\Delta\omega$, $\pm\chi$ in the

range $0° < |\chi| < 90°$. For $|\chi| > 90°$ the $\Delta\phi$ expression gives the correct result, but the negative supplement of χ (χ - 180°) must be used in the $\Delta\chi$ computation. The general nature of the functions are summarized in Table 7.

Table 7. The nature of the general tuning expressions

χ	$\Delta\omega$	$\Delta\phi$	$\Delta\chi$
>90°	+	+	+
	-	-	-
+90°	+α	+ or - 90°	+ or - α
	-α	+ or - 90°	- or + α
0° < χ < 90°	+	-	-
	-	+	-
0°	+α	-α	0°
	-α	+α	0°
-90° < χ < 0°	+	-	+
	-	+	+
-90°	+α	+ or - 90°	- or + α
	-α	+ or - 90°	+ or - β
<90°	+	+	-
	-	-	-

The general tuning algorithm is therefore followed by rotating omega to equal theta and then calculating the required compensating $\Delta\chi$ and $\Delta\phi$ using expressions IV and XI, respectively.

Implementation of this algorithm has been made on a Hilger and Watts four-circle x-ray diffractometer. A comparison of the experimental findings with the calculated corrections for a particular reflection is presented in Table 8. Not only is the appropriatness of the expression verified, but also credit is made to the sensitivity of the instrument.

Table 8. Comparison of calculated and observed angle settings for a tuned reflection at $\theta = 8.462°$

Run	Omega tuned[a]	Chi tuned[a]	Phi	$\Delta\phi$ calc.[b]	$\Delta\phi$ obs.[c]	$\Delta\chi$ calc.[d]	$\Delta\chi$ obs.[e]
1	8.601	62.190	74.700	0.298	--	0.0	--
2	8.535	62.039	254.700	0.156	--	0.0	--
3	7.665	62.212	76.700	-1.709	-1.702	-0.011	-0.022
4	7.593	62.048	256.700	-1.853	-1.844	-0.013	-0.009
5	3.722	62.590	85.200	-10.210	-10.202	-0.376	-0.400
6	3.645	62.431	265.200	-10.341	-10.344	-0.387	-0.392

[a]The tuned omega and chi values are averages of three experimental tunings of the reflections for runs 1, 2, 5 and 6 and are averages of four tunings for runs 3 and 4. The estimated standard deviations are $\pm 0.010°$ for omega and $\pm 0.03°$ for chi.

[b]Calculation made by means of expression IV.

[c]$\Delta\phi = \phi_{1 \text{ or } 2}$ (calc.) - ϕ (obs.).

[d]Calculation made by means of expression XI.

[e]$\Delta\chi = \chi_{1 \text{ or } 2}$ (calc.) - χ(obs.).